Trends in Analytical Chemistry 143 (2021) 116349

Contents lists available at ScienceDirect

Trends in Analytical Chemistry

journal homepage: www.elsevier.com/locate/trac

Aptamers against viruses: Selection strategies and bioanalytical applications

Elena Sánchez-Báscones [a], Francisco Parra [a, b, c], María Jesús Lobo-Castañón [a, b, d, *]

[a] Instituto Universitario de Biotecnología de Asturias, Universidad de Oviedo, Edificio Santiago Gascón, Campus del Cristo, 33006, Oviedo, Spain
[b] Instituto de Investigación Sanitaria del Principado de Asturias, Avenida de Roma, 33011, Oviedo, Spain
[c] Dpto. Bioquímica y Biología Molecular, Universidad de Oviedo, Edificio Santiago Gascón, Campus del Cristo, 33006, Oviedo, Spain
[d] Dpto. Química Física y Analítica, Universidad de Oviedo. Av. Julián Clavería 8, 33006, Oviedo, Spain

ARTICLE INFO

Article history:
Available online 3 June 2021

Keywords:
Aptamers
Viruses
SELEX
Aptasensors
Viral detection

ABSTRACT

Viruses are infectious agents that can only replicate inside cells. Tests available to make an early and effective diagnosis of viral diseases are mainly based on PCR, the gold-standard method, or in the detection of virus antigens or antibodies against them. The need for rapid diagnostic tests postulates aptamers as an alternative to antibodies. Aptamers are short single-stranded nucleic acid molecules that are selected through an *in vitro* process called SELEX. They show numerous advantages over antibodies, such as greater stability and chemical synthesis that minimizes variability between batches. However, they still have some limitations, for example, their low commercial availability, or the absence of standardized protocols for their characterization. In this work, different approaches for selecting aptamers against viruses are presented, as well as their targets, sequences, and binding affinities. Recent efforts aimed to develop aptamer-based methods for viral detection, using optical, electrochemical and piezoelectric transduction, are critically reviewed.

1. Introduction

Emerging infectious diseases, previously unknown or known but rapidly increasing in incidence or geographic range, exert a tremendous impact on global health and economies [1]. Among the pathogens causing such diseases, viruses play a prominent role making up over two-thirds of all new human pathogens, most of them of zoonotic origin [2]. As an example, the virus SARS-CoV-2 (*severe acute respiratory syndrome coronavirus 2*), the causative agent of the COVID-19 declared as pandemic by the WHO on March 11, 2020. It marks a return to an old problem largely ignored. Like this virus, there could be millions of undiscovered viruses that might constitute future health threats that should be readily and specifically detected and treated.

Throughout history, there have been different viral outbreaks and epidemics, which killed millions of people (Table 1). From the 1520 smallpox epidemic in the Aztec Empire to the current COVID-19 pandemic, multiple viruses including *influenza viruses*, *human immunodeficiency viruses* (HIV), *Ebola virus* (EBOV) or *coronaviruses* caused severe public health threats and pushed the scientific community to develop new therapies and diagnostic tools.

The ideal test for the diagnosis of viral infections must be cheap, fast, accurate, sensitive, specific, and easy to use. The methods currently used for this purpose are classified into two categories: indirect and direct measurements. The indirect methods or serology tests detect specific antiviral antibodies. The direct ones are based on viral isolation by cell culture or the detection of virus components i.e. nucleic acids, usually by PCR, or viral antigens [3]. Most of these methods require specialized personnel and relative expensive instrumentation. To date mainly serology and antigen tests, based on immunoassays, have seen a slow transition to the point of care. These tests require the obtention of specific antibodies, a long and expensive process that often leads to batch-to-batch variations.

A likely superior approach would take advantage of alternative synthetic receptors that can be obtained more quickly, at lower cost and by chemical synthesis, reducing batch variations. Motivated by these needs, significant recent effort has focused on the development of aptamers that could be useful not only to develop diagnostic assays but also as agents in antiviral therapy [4]. To facilitate the

* Corresponding author. Dpto. Química Física y Analítica, Universidad de Oviedo. Av. Julián Clavería 8, 33006, Oviedo, Spain
E-mail address: mjlc@uniovi.es (M.J. Lobo-Castañón).

https://doi.org/10.1016/j.trac.2021.116349

growth of these efforts, we review here the published approaches for selecting aptamers against viruses, collecting the full sequences of the antiviral aptamers selected so far. These data are not usually found in databases. Furthermore, detailed information will be provided on the experimental conditions under which aptamers were selected and their affinity characteristics. This information is very useful, not only for the development of new methods to detect, identify and monitor viruses in clinical samples, but also as a guide for the development of aptamers against new viruses. Aptamers have been coupled to different transducers to obtain cost effective devices useful for early diagnostic of viral diseases. This review will then focus in the most commonly used aptamer-based strategies for the detection of human viruses in clinical samples.

In recent years, numerous reviews on aptamer selection and applications have been published [4–14]. Many of them describe the applications of aptamers in biomedical diagnosis [8,13,14] or focus on a specific disease such as cancer [6]. Among the reviews focused on antiviral aptamers, most of them describe their applications either in diagnostics [9,11] or therapy [5], with limited information about the aptamer selection targets and sequences. In this review, we summarize the different SELEX (Systematic Evolution of Ligands by EXponential enrichment) variants used for selecting aptamers against human viruses, analyzing their applications in diagnosis, and highlighting the unrealized potential and opportunities in this field.

2. Selection of aptamers against viral targets

Aptamers are short synthetic single-stranded nucleic acids, either ssDNA or RNA with typically less than 100 nucleotide residues, capable of binding to a specific target with high affinity and selectivity. They are selected from highly complex libraries of nucleic acids manufactured by combinatorial synthesis, through an *in vitro* enrichment process called SELEX, which was first described in 1990 by two independent laboratories [15,16]. The first described aptamers were RNA molecules for specifically recognizing organic dyes [15] or the bacteriophage T4 DNA polymerase [16]. Later in 1992, it was demonstrated that using a similar method it is also possible to isolate DNA aptamers [17]. In the same year, the laboratory of Prof. Gold described the first RNA aptamer with potential therapeutic activity against viral infections, which acted as specific inhibitor of the reverse transcriptase of *human immunodeficiency virus* type 1 (HIV-1) [18]. Very soon after, an RNA aptamer able to neutralize an avian retrovirus, the *Rous sarcoma virus*, was selected [19], without knowing the structures of the viral proteins. The first ribonuclease-resistant aptamer for the recognition of a human infective virus was described in 2000 against *human cytomegalovirus* [20]. Since then, a diversity of aptamers for recognizing a great variety of human viruses have emerged, as shown in Fig. 1A, where viruses studied are classified according to different criteria: the nature of genome (RNA or DNA), the symmetry of their protein shell (capsid), the presence or absence of a lipid membrane or envelope, the genome architecture, and the Baltimore classification providing information about their replication mechanism.

The scheme of a SELEX is depicted in Fig. 1B; it is an *in vitro* and iterative process that involves the following general steps: interaction between the starting library of randomized oligonucleotides and the selected target in a suitable milieu, separation of bound from unbound oligonucleotides, elution of the target-bound oligonucleotides to isolate the highest binders, followed by amplification of these binders by PCR, and conditioning to obtain a new pool of single-stranded oligonucleotides, with lower variability than the starting mixture, which is enriched in molecules recognizing the target with high affinity and selectivity. The process is repeated for several rounds under increasingly stringent interaction conditions until the enrichment is considered sufficient. The sequences in the last pool are identified by cloning and sequencing or using next generation sequencing. To efficiently select anti-virus aptamers, we highlight in the following sections the key factors to consider in each of these steps, including post-SELEX modifications that ensure maximum stability and cost-efficiency.

2.1. Design of the starting library

The input library is typically a mixture of 10^{13} to 10^{15} DNA oligonucleotide sequences that are chemically synthesized and consist of a random central region of defined length flanked by known sequences for primer binding [21]. There are no rules for choosing the length of the random region, typically between 20 and 80 residues, limited by the low yields in the synthesis of longer oligonucleotides. The SELEX for obtaining antiviral aptamers described so far use oligonucleotide libraries with a central part that ranges between 15 and 74 nucleotides in length (Table 2). When RNA aptamers are desired, the starting library is generated by *in vitro* transcription of the synthetic DNA templates using a T7 RNA polymerase. In order to guarantee the maximum variability, it is recommended that the random region contains equimolar amounts of the four nucleotides [10]. The rationale behind this recommendation is that binding to the target is commonly associated to short motifs, and an equal distribution of bases increases the probability of even motif dispersion and consequently a greater probability of success in the selection. In some cases, a biased library has been used in order to improve the binding region of previously selected aptamers using a conventional library [22]. This work used a partially randomized (doped) sequence of an RNA aptamer against *human influenza virus* H3N2 at a 37.5% mutation rate, which meant that every randomized position contained 62.5% of wild-type nucleotide and 12.5% of each other nucleotide, to

Table 1
Some of the viral outbreaks and epidemics that have occurred throughout history.

Year	Disease	Observations
1520	Smallpox	An epidemic that reduced the population of Tenochtitlan by 40% in one year, contributing to the fall of the Aztec Empire
1918	Flu	A pandemic caused by an influenza virus that spread around the world in one year, causing some 50 to 100 million deaths
20th century	HIV/AIDS	A pandemic still with us, which has killed an estimated 32 million people since its start in 1981
2003	SARS	The first epidemic caused by a *coronavirus*, the *severe acute respiratory syndrome-coronavirus 1* (SARS-CoV-1), which started in China and spread to 26 countries
2009	Influenza A	The first global influenza pandemic of the 21st century
2012	MERS	Epidemic caused by a novel *coronavirus* (*Middle East respiratory syndrome coronavirus*, or MERS-CoV) that was first identified in Saudi Arabia and spread to 27 countries
2014	Ebola	The largest, most severe and most complex outbreak of *Ebola virus* (EBOV) disease, with more than 28,000 people infected, and over 11,000 deaths
2019	COVID-19	The third, most dangerous and severe infection caused by a *coronavirus*

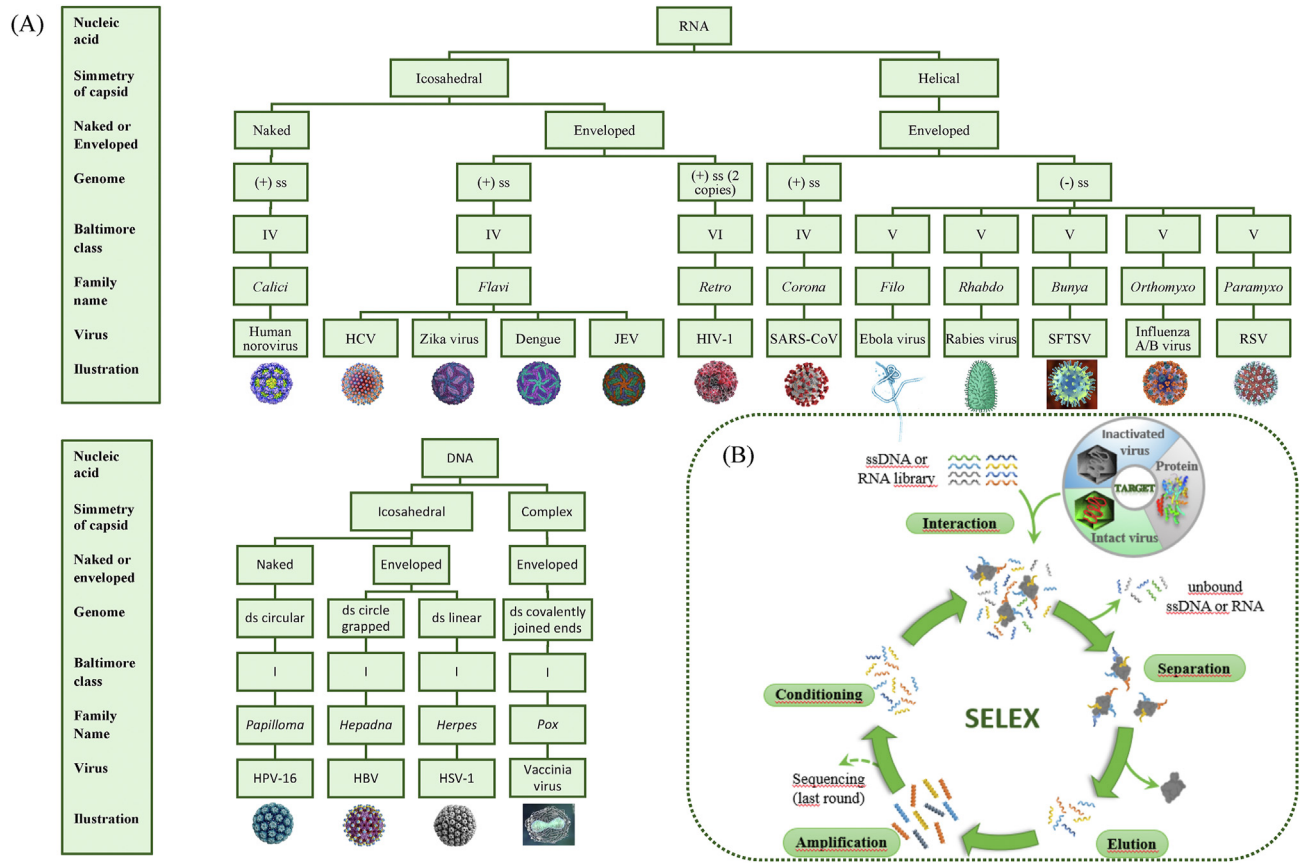

Fig. 1. (A) Classification of virus against which aptamers have been efficiently selected. (B) Scheme of the steps involved in the selection of aptamers.

obtain new aptamers with improved affinity. A similar strategy but with lower mutation percentage has been used to improve the affinity of aptamers against HIV-1 [23]. The randomized sequence can also be segmented in order to impose structural constraints to the final aptamer, thus reducing the number of selection cycles [24].

Degradation of aptamers by nucleases is one of the main issues in terms of stability, especially for RNA aptamers. To improve the resistance to degradation, it is possible to use libraries that incorporate unnatural nucleotides, which differ from the natural ones in at least one of their moieties (the nucleobase, the ribose or the phosphate backbone) giving rise to xeno-nucleic acids (XNA) with enhanced resistance to nucleases. Some of this XNA can be processed by natural polymerases, but in most cases, they require the use of specially engineered enzymes. The use of a T7 RNA polymerase optimized for incorporating pyrimidine nucleosides modified at the 2′-position of the ribose moiety with a fluoro group (2′-F-dUTP and 2′-F-dCTP) allowed the direct selection of high affinity F-RNA aptamers for the recognition of HIV-1 [25–27]; *severe acute respiratory syndrome coronavirus*, SARS-CoV [28]; *hepatitis C virus*, HCV [29] or EBOV [30]. In a similar way, an aptamer was raised to *Japanese encephalitis virus*, JEV [31] using a library containing 2′-O-methyl pyrimidines.

The list of XNA is continuously growing with the goal of not only improving stability, but also expanding the chemical functionality of nucleic acids and increasing aptamer binding affinity. Synthetic libraries containing 2′-deoxy-2′-fluoroarabino-nucleotides, FANA, led to aptamers with picomolar affinity against HIV-1 reverse transcriptase [32] and HIV-1 integrase [33]. These aptamers are characterized by a structure different from that of the 2′-fluororibonucleotide-containing aptamers because the sugar adopts a C2′/O4′-endo conformation versus the C3′-endo conformation for 2′-fluororibonucleotides, with the fluorine group in the β conformation (as opposed to α conformation of RNA or F-RNA).

Chemical modifications can also be included in the nucleobases, as an example (E)-5-(2-(N-(2-(N6-adeninyl)ethyl))calbamylvinyl)-2′-deoxyuridine-5′-triphosphate ($dU^{ad}TP$) has been included in the library for the selection of aptamers capable of recognizing EBOV [34]. In this context, Prof. Gold's team described a new class of aptamer, the Slow Off-rate Modified Aptamers (SOMAmers) [35], which are DNA aptamers including different 2′-deoxyuridine nucleotides with modifications on the C5 position of the base. Different residues have been added to the uracil moiety, mimicking the structural diversity of amino acids. SOMAmers targeting HCV [36] and *human papilloma virus* type 16, HPV-16 [37] have been successfully selected. Despite these modifications improve the affinity of the obtained aptamers, exclusive intellectual property rights by SomaLogic (Boulder, CO) limit the application of SOMAmers.

2.2. Selection of the target

Several targets have been used for the efficient selection of aptamers against human viruses. In many cases a predefined and well-characterized molecule is used, typically an epitope of the viral pathogen. In this sense, structural proteins from the virus capsid or the envelope, such as hemagglutinin (HA) for the *influenza B* and *A virus* [38,39], the core and E2 proteins for HCV [36,40], the glycoprotein gp120 of HIV-1 [25] and N protein for SARS-CoV [28] have been isolated or obtained in a recombinant process to be used as target for the selection. In some cases, a specific domain or region of the protein is preferred in order to modulate the

Table 2
Summary of aptamers selected against viral antigens.

Virus	Target	Selection conditions (binding buffer)	Aptamer sequence[a] (5'→3', central region flanked by underlined conserved sequences) (length of the random region of the initial library)	K_D/nM	Reference
Human NoV	VLP	PBS[b] (pH 7.1), 100 mg/L $CaCl_2$, 100 mg/L $MgCl_2$, 0.05% Tween 20[c]	(SMV-25) AGTATACGTATTACCTGCAGCCATCTGTGTGAAGACTATATGGCGCTCACAT ATTTCTTTCCGATATCTCGGAGATCTTGC	232	[49]
			(SMV-21) AGTATACGTATTACCTGCAGCCCATGTTTTGTAGGTGTAATAGGTCATGT TAGGGTTTCTGCGATATCTCGGAGATCTTGC (N_{40})	101	
HCV	Recombinant E2 glycoprotein	–	(E2-A) GGCUGGUGGUGUGGCUGCUUUAUGCGUUUGCCUCGGAGUUUGGAGAGA CUCGGCCCAGGCAGACGGUCACUC	0.8–4	[36]
			(E2-B) GGCUGGUGGUGUGGCUGAUUAGACCCAUUGCCAUUUUAUCAUUAAUUU AUACCGUGCCAGGCAGACGGUCACUC		
			(E2-C) GGCUGGUGGUGUGGCUGUCGAGCUUUAUGCGUUUGCCUCGGAGUUUGCG AGCGGAACAGGCAGACGGUCACUC		
			(E2-D) GGCUGGUGGUGUGGCUGAAACGUGGGUGGUUUGGUGGGGGUUGGUGGG UGGGUUUACAGGCAGACGGUCACUC		
			(U represents 5-benzylaminocarbonyl-dUridine, BzdU) (SOMAmers) (N_{40})		
HCV	Recombinant core protein	50 mM Tris[d]-Cl (pH 7.6), 200 mM potassium acetate, 5 mM $MgCl_2$, 2.5 mM DTT[e]	(9–15) AGCAUGGAUCGAGGAUGGGAACACCCAGUAG GAGGAUGGGCAUGGCCGGACCCAAAAUUAGCAGUGGGACAGUACUCAGGUCAUCC UAGG (N_{60})	224	[40]
HCV	Recombinant NS5B polymerase	50 mM Tris-Cl (pH 7.5), 100 mM KCl, 50 mM NaCl, 5 mM $MgCl_2$	(B.1) UGCCGUGCCGUAUGGACCAGUGGCCGGCUUCGGCCCCAAUGUCUG	3	[24]
			(B.2) CGAAGCCGCUAUGGACCAGUGGCGCGGCUUCGGCCCGACGGAGUG (Underlined non-random regions of the central region) (N_{35})	1.5 ± 0.2	
HCV	Recombinant NS5B polymerase	–	(R–F) GGGAGAGCGGAAGCGUGCUGGGCCUUGAACGAUUGGUAGUAGAAUAUCGUC AGUGAACGGCAGUCAUAACCCAGAGGUCGAUGGAUCCU	6.73 ± 0.50	[29]
			(R–F t2) UUGAACGAUUGGUAGUAGAAUAUCGUCAG	2.62 ± 0.90	
HCV	Recombinant NS5B polymerase	20 mM Tris (pH 7.5), 5 mM $MgCl_2$, 1 mM DTT, 100 mM NaCl	(27v) ACGTACACTAGTGGTCCGGGCGGGGCTCATTGTCC (N_{35})	98 ± 2	[57]
HCV	NS3 domain of the recombinant helicase	30 mM Tris-HCl (pH 7.5), 150 mM NaCl, 1.5 mM $MgCl_2$, 2 mM DTT, 1% BSA[f]	(#1) GGGAGAGCGGAAGCGUGCUGGGCCAGUAGUGUAUAGGGCUCGAAAUGUUCAUG GCUCAGUGGACAUAACCCAGAGGUCGAUGGAUCCCCCC	0.990	[87]
HCV	Cells with the E2 glycoprotein expressed on their surface	25 mM Tris-HCl, 50 mM KCl, 200 mM NaCl, 0.2 mM EDTA[g], 5% (v/v) glycerol, 0.5 mM DTT	(ZE2) GCGGAATTCTAATACGACTCACTATAGGGAACAGTCCGAGCCGAATGAGGAATAAT CTAGCTCCTTCGCTGAGGGTCAATGCGTCATA (N_{30})	1.05 ± 0.4	[47]
ZIKV	Recombinant NS1 protein	20 mM Tris (pH 7.5), 150 mM NaCl, $MgCl_2$ 1 mM, 2.7 mM KCl, 0.005% NP-40	2) GATAGAATTCGAGCTCGGGCACTAGGTTGCAGGGGACTGCTCGGGATTGCGGATCAAC CTAGTTGCTTCTCTCGTATGATGCGGGTCGACAAGCTTTAAT	0.024	[69]
			(10) GATAGAATTCGAGCTCGGGCCGGCTGTTGTTGTTACCTATTGCGTGGCGATCGGACTTTCG ATTCCGATTAACGCCGGAGGGCGGGTCGACAAGCTTTAAT (N_{60})	134	
DENV-2	Recombinant methyltransferase	30 mM Tris-HCl (pH 7.5), 150 mM NaCl, 1.5 mM $MgCl_2$, 2 mM DTT, 1% BSA	(truncated aptamer 3) GGUUGGGCACAUAUAGACUGUGUAAUUCGUAUAGUGUGC AUAACC (N_{40})	28 ± 2.1 (serotype 2) 15.6 ± 1.2 (serotype 3)	[71]
DENV-2	Recombinant envelope protein 3 domain	50 mM K_2HPO_4, 100 mM NaCl, 0.1 mM EDTA, pH 6.5	(S22) GGGAAGATCTCGACCAGAAGCCGCACCACATCAGCCCGTCGTCGCCCTCGTCCGGC ATATGTGCGTCTACATGGATCCTCA	500	[72]
			(S15) GGGAAGATCTCGACCAGAAGGCACCGGGCAGGACGTCCGGGGTCCTCGGGGGGGTATG TGCGTCTACATGGATCCTCA (N_{35})	200	
JEV	Methyltransferase domain of NS5 protein	30 mM Tris-HCl (pH 7.5), 150 mM NaCl, 1.5 mM $MgCl_2$, 2 mM DTT, 1% BSA	(G2) GGGAGAGCGGAAGCGUGCUGGGCCCCACGACAGCAUGCCAAUAGAUGCGCAUGG AGACGACAGCAUCAUAACCCAGAGGUCGAUGGAUCCCC	13 ± 2	[31]
			(Truncated G2) GAUGCGCAUGGAGACGACAGCAUC (C/U indicates 2′-O-methyl modified nucleotides) (N_{40})	16 ± 3	
HIV-1	gp120 Glycoprotein	10 mM HEPES[h] (pH 7.4), 150 mM NaCl, 1 mM $CaCl_2$, 1 mM $MgCl_2$, 2.7 mM KCl	(B4) AAUUAACCCUCACUAAAGGGAACUGUUGUGAGTUCUCAUGUCGAAGAGCGGUU AAGGGAGAUUUAGGCAGCAGCUUGGACAGUGUAUCGGCUGAGUUGAGCGUCU AGUCUUGUCU	–	[25]
			(B40) AAUUAACCCUCACUAAAGGGAACUGUUGUGAG TUCUCAUGUCGAAUGUGGGC CACGCCCGAUUUUACGCUUUUACCCGCACGCGAUUGGUUUGUUUUGAGCGUCUAGU CUUGUCU (F-RNA aptamers) (N_{49})		

HIV-1	gp120 Glycoprotein	10 mM HEPES (pH 7.4), 50 −150 mM NaCl, 1 mM $CaCl_2$, 1 mM $MgCl_2$, 2.7 mM KCl, 10 mM DTT, 0.01% BSA	(A-1) GGGAGGACGATGCGGAATTGAGGGACCACGCGCTGCTTGTTGTGATAAGCAGTTTGTC GGATGGCAGACGACTCGCCCGA (DNA sequence shown although the selection is made for F-RNA aptamers) (N_{50})	52	[27]
HIV-1	Mutated integrase	20 mM Tris-HCl (pH 7.5), 200 mM NaCl, 6 mM $MgCl_2$, 1 mM DTT	(IN 1.1) AAAAGGTAGTGCTGAATTCGUUUCAAGUGUAUAUUAACUACGCAUCUUUCCCCCUGC GUAUUCGCUAUCCAGUUGGCCU (DNA-FANA chimera, being FANA 2′-fluoroarabinonucleic acid) (N_{40})	~0.050−0.100	[33]
HIV-1	Recombinant integrase	PBS (pH 7.4), 1 mM $CaCl_2$, 2.7 mM KCl, 2 mM $MgCl_2$	(S3R3) TAATACGACTCACTATAGGGAGGACGATGCGGGCGGAGGACGAUGCGGGCCGUCGUA UGCUGCGCCAUGGGGUGGACUGGGUGGCGCGAGAGGUGGGTGGC GCGAGAGGTG (N_{30})	–	[43]
HIV-1	Recombinant reverse transcriptase	HRT buffer	(RT12) ATCCGCCTGATTAGCGATACTCGATTAGGTCCCCTGCCGCTAAACAGCGCCGCGGTAACT TGAGCAAA ATCACCTGCAGGGG	2	[45]
			(RT26) ATCCGCCTGATTAGCGATACTTACGTGAGCGTGCTGTCCCCTAAAGGTGATACGTCACTT GAGCAAAATCACCTGCAGGGG	1	
			(RT1t49) ATCCGCCTGATTAGCGATACTCAGAAGGATAAACTGTCCAGAACTTGGA (N_{35})	4	
HIV-1	Recombinant reverse transcriptase	50 mM Tris-HCl (pH 8), 80 mM KCl, 2 mM $MgCl_2$, 1 mM DTT	(FA1) AGGCCAACTGGATAGCGAAAAAGGTAGTGCTGAATTCGGGGCCATTAAGATATTCGTCGA AGTTCGGTT GTTTCCCTTCGCTATCCAGTTGGCCTCGAATTCAGCACTACCTTTTGGCAAA (FANA aptamer, being FANA 2′-fluoroarabinonucleic acid) (N_{40})	$(4 \pm 3) \cdot 10^{-3}$	[32]
HIV-1	Ribonuclease domain of the recombinant reverse transcriptase	50 mM Tris-HCl (pH 7.9), 6 mM Mg^{2+}, 10 mM DTT	(ODN93) CCCCTGCAGGTGATTTTGCTCAAGTGGGGGTGGGAGGAGGGTAGGCCTTAGGTTTCTG AAGTATCGCTAATCAGGCGGATA (N_{35})	–	[44]
HIV-1	Recombinant protease	20 mM HEPES (pH 7.4), 150 mM NaCl, 5 mM $MgCl_2$	(PR10.1) GGGUUACCUAGGUGUAGAUGCUCUUCAUUGUAACUUCUCAUAAUUUCCCGAGGCU UUUACUUUCGGGGUCCUAAGUGACGUCUGAACUGCUUCGAA	115 ± 22	[23]
			(PR10.1−8A) GGGUUACCUAGGUGGAGAUGCUCUUAAGUGUAACUUCUCGUAAUUCCCAAGGC UUUUACCUCGGGGUCCUAAGUGACGUCUGAACUGCUUCGAA (N_{50})	2.2 ± 0.2	
HIV-1	Enveloped pseudovirus	–	(CSIR1.1) TAATACGACTCACTATAGGGAGACAAGACTAGACGCTCAACCCCGAAGATGCCTTCAT GAGCGCACCATCTTGCCACCGACTTCAAATTCGACATGAGACTCACAACAGTTCCCTTTAGTGAGG GTTAATT (DNA sequence shown although the selection is made for F-RNA aptamers) (N_{50})	16 ± 6	[26]
SARS-CoV-1	Nucleocapsid N protein	50 mM Tris-Cl (pH 8.0), 150 mM NaCl, 1.5 mM $MgCl_2$, 2 mM DTT, 1% (w/v) BSA	(1) GCAATGGTACGGTACTTCCGGATGCGGAAACTGGCTAATTGGTGAGGCTGGGGCGGTCGTG CACAAAAGTGCACGCTACTTTGCTAA (N_{45})	4.93 ± 0.30	[88]
SARSCoV-1	Nucleocapsid N protein	30 mM Tris-HCl (pH 7.5), 150 mM NaCl, 10 mM MgCl2, 2 mM DTT, 1% BSA	(1) GGGAGAGCGGAAGCGUGCUGGGCCUGUCGUUCGCUGUCUUGCUACGUUACGUUACACG GUUGGCAUAACCCAGAGGUCGAUGGAUCCCCCC (2′-deoxy-2′-fluoro C and U, F-RNA aptamers) (N_{40})	1.65 ± 0.41	[28]
SARS-CoV-2	Receptor-binding domain (RBD) of the spike glycoprotein	PBS, 0.55 mM $MgCl_2$	(CoV2-RBD-1C) CAGCACCGACCTTGTGCTTTGGGAGTGCTGGTCCAAGGGCGTTAATGGACA	5.8 ± 0.8	[79]
			(CoV2-RBD-4C) ATCCAGAGTGACGCAGCATTTCATCGGGTCCAAAAGGGGCTGCTCGGGATTG CGGATATGGACACGT (N_{40})	19.9 ± 2.6	
EBOV	Recombinant nucleoprotein and glycoprotein	20 mM HEPES (pH 7.4), 150 mM NaCl, 2 mM KCl, 2 mM $MgCl_2$, 2 mM $CaCl_2$	(GP-D01) AGCAGCACAGAGGTCAGATGGCCGCAGACAGAAACACAAACAGTATACAGCTATCTC GCTTGGACCTCGCATAATATACGCCTATGCGTGCTACCGTGAA	4.1 ± 0.9 glycoprot.	[66]
			(NP−C04) AGCAGCACAGAGGTCAGATGGTTGGGGTTAGGGTGAATATCCCCTCGCTATGATCTCGGTGACG TCAAATGATTATTTTTCCTATGCGTGCTACCGTGAA (N_{60})	8.1 ± 2.4 nucleoprot.	
EBOV	Soluble glycoprotein	137 mM NaCl, 2.7 mM KCl, 10 mM Na_2HPO_4, 2 mM KH_2PO_4, 5 mM $MgCl_2$, pH 7.4	(5183) GGGAGACAAGAAUAAACGCUCAAUUUUUUAUUGCAUUUUUCUUUGAGCGUCAUUG AUACCCUGUUUCCUUGAGCAGUUCGACAGGAGGCUCACAACAGGC (F-RNA aptamers) (N_{53})	54	[30]
EBOV	Recombinant protein 24	20 mM Tris-HCl (pH 7.40), 1 mM $MgCl_2$, 10 mM NaCl, 0.05% Tween 20	(VPNA1) TCGCCTTGCCGGATCGCAGAGACCCTCTGGGCATCGCCGCTTAGGACGCGTGGTCCGT GAGCCTGACACC	8.3 ± 2.9	[34]
			(VPKS-5) TCGCCTTGCCGGATCGCAGAAGCG**T**G**T**AAAC**T**ACG**T**CGCAGCGAACACCC**T**GG**T**CCG**T**GAGCC**T**G ACACC (dU^{ad} modified nucleotides in bold) (N_{30})	0.23 ± 0.13	
EBOV	Recombinant protein 23	–	(1G8-14) GGGAGACAAGAAUAAACGCUCAAGGCAUUUCUGCUAGUCUGGUUGUAAGAUAUU CAACACGUGAGUUUCGACAGGAGGCUCACAACAGGC	10−50	[51]
			(2F11-14) GGGAGACAAGAAUAAACGCUCAACGUUCA GUAUAACAGUCCGAGUCUAACACACAAUGGGACACUGAAUUCGACAGGAGGCUCAC AACAGGC (N_{45})		
RABV	Cells with the virus glycoprotein expressed on their surface	4.5 g/L Glucose, 5 mM $MgCl_2$, PBS, yeast tRNA, 1.0 g/L BSA	(GE54) TATTTTTATATTTGTTTGACAGTCGCTTGCTTGTGTAGGCGTT	307	[48]
			(GE58) TTAATTTTTTGATCTTTGATTGTTTTATTTTTTTTATTGTTTGTG	475	
			(GT1) TTCTGGTGTGGTAACTCATGTATCGGTCGTGGGGGTCGTGGCATT (N_{45})	395	

(*continued on next page*)

Table 2 (*continued*)

Virus	Target	Selection conditions (binding buffer)	Aptamer sequence[a] (5'→3', central region flanked by underlined conserved sequences) (length of the random region of the initial library)	K_D/nM	Reference
SFTSV	Recombinant nucleocapsid protein	50 mM Tris-HCl (pH 7.4), 100 mM NaCl, 5 mM KCl, 1 mM $MgCl_2$, 0.01% Tween 20	(SFTS-apt 3) ATCCAGAGTGACGCAGCACACATCGGAG AACAGGCGCACTGTCGGAGGAACCGCAACGTGGACACGGTGGCTTAGT (N_{40})	800 ± 200	[64]
Influenza A virus	HA globular region	50 mM Tris-HCl (pH 7.4), 5 mM KCl, 100 mM NaCl, 1 mM $MgCl_2$, 100 μg tRNA, 0.2% BSA	(A22) AATTAACCCTCACTAAAGGGCTGAGTCTCAAAACCGCAATACACTGGTT GTATGGTCGAATAAGTTAA (N_{30})	55.7 ± 10.9	[41]
Influenza A virus H1Nx	Recombinant HA	50 mM Tris-HCl (pH 8.0), 150 mM NaCl, 1.5 mM $MgCl_2$, 2 mM DTT, 1% (w/v) BSA	(ApI) GCAATGGTACGGTACTTCCGGGTGGGTGGGAGGGGGTGGAGGTTGGGGGTTGGACGCA GAGTGCCAAAAGTGCACGCTACTTTGCTAA	65 ± 18	[39]
			(ApII) GCAATGGTACGGTACTTCCTCGTGTGGGGTGGGTGTTGTGGGGGTGGGTGGGTGGGCTC GGGCGCAAAAGTGCACGCTACTTTGCTAA	69 ± 12	
			(ApIII) GCAATGGTACGGTACTTCCGGGTGGGCAGGAGGGGGTGGGCGGGTGGGGGGTCGCAA TAGCGTCCAAAAGTGCACGCTACTTTGCTAA (N_{45})	50 ± 14	
Influenza A virus H1N1	Inactivated virus	PBS (pH 7.4)	GGCAGGAAGACAAACAGCCAGCGTGACAGCGACGCGTAGGGACCGGCATCCGCGGGTGGTCTG TGGTGCTGT (N_{40})	55 ± 20	[65]
Influenza A virus H1N1	Inactivated virus	PBS, 5 mM $MgCl_2$	(A20S) GCAATGGTACGGTACTTCCGGACCAGTTGTCTTTCGGTCTCTACCCCAGCCCGTCAAAA GTGCACGCTACTTTGCTAA (N_{35})	6 ± 4	[61]
Influenza A virus H1N1	Recombinant HA	50 mM Tris-HCl (pH 7.4), 100 mM NaCl, 5 mM KCl, 1 mM $MgCl_2$, 0.01% Tween 20	(RHA0006) GGGTTTGGGTTGGGTTGGGTTTTTGGGTTTGGGTTGGGTTGGGAAAAA (RHA0385) TTGGGGTTATTTTGGGAGGGCGGGGGTT (RHA1635) GGGGCCCACCCTCTCGCTGGCGGCTCTGTTCTGTTCTCGTCTCCTTGATTTC TGTGGGCCCC Also recognized H3N2 and H5N1 (N_{30})	15.3	[75]
Influenza A virus H1N1	Recombinant HA	20 mM HEPES[f] (pH 7.35), 120 mM NaCl, 1 mM $MgCl_2$, 1 mM $CaCl_2$, 5 mM KCl	(1) GGGAGCTCAGAATAAACGCTCAAGGCACGGCATGTGTGGTATGTGGTGCCTGTACTCG TTCGACATGAGGCCCGGATC (N_{35})	78 ± 1	[63]
Influenza A virus H1N1	Recombinant HA	50 mM Tris-Cl (pH 7.4), 5 mM KCl, 100 mM NaCl, 1 mM $MgCl_2$	(A10) GAATTCAGTCGGACAGCGGGGTTCCCATGCGGA TGTTATAAAGCAGTCGCTTATAAGGGATGGACGAATA TCGTCTCCC (N_{40})	–	[76]
Influenza A virus H1N1	Recombinant HA and intact virus	–	(V46) TACTGCACACGACACCGACTGTCACCATCACCTCGGCGCA (N_{40})	19.2 ± 5.7	[68]
Influenza A virus H3N2	Intact virus	20 nM HEPES/KOH (pH 7.4), 105 mM NaCl	(P30-10-16) GGGAGAAUUCCGACCAGAAGGGUUAGCAGUCGGCAUGCGGUACAGACAG ACCUUUCCUCUCUCCUUCCUCUUCU (N_{30})	0.188 (HA)	[53]
Influenza A virus H3N2	HA	0.01 M HEPES (pH 7.4), 0.15 M NaCl, 3 mM EDTA, 0.005% Tween 20	(Clone A) GGGAGAAUUCCGACCAGAAGGGUUAGCA**GUCG**G**C**A**U**GCG**GUA**CAGACAGACCU UUCCUCUCUCCUUCCUCUUCU	~0.200	[22]
			(Clone B) GGGAGAAUUCCGACCAGAAGGGUUAGCG**GUCG**U**CUU**AA**GUA**GUUUUUGGU CCUUUCCUCUCUCCUUCCUCUUCU(Nucleotides of the consensus sequence, 5′-GUCGN CNU$(N)_{2-3}$GUA-3′, for HA recognition in bold) (N_{30})	0.12 ± 0.03	
Influenza A virus H5Nx	Intact virus	–	(IF22, H5N1) CGTACGGTCGACGCTAGCTAAATGGGCG TGGGAATGACTCTACGGGGCCACGTGGAGCTCGGATCC (IF23, H5N8) CGTACGGTCGACGCTA GCGCCAAAAGTGGGTGGCGGTGGGTATGCTCCACGTGGAGCTCGGATCC (IF20, H5N1 and H5N2) CGTACGGTCGACGCTAGCAGGGGTAGCGCTACAGAGGGGAACATAG GTCACGTGGAGCTCGGATCC (IF15, H5N1 and H5N8) CGTACGGTCGACGCTAGCAGGTGTGGGTTGTTCTGGTCGACTGTGAT GCACGTGGAGCTCGGATCC (IF10; H5N1, H5N2 and H5N8) CGTACGGTCGACGCTAGCTAACGGTGTGGCCCGGGGGTACAG CGCACTCACGTGGAGCTCGGATCC (N_{30})	$1 \cdot 10^4$–$8 \cdot 10^4$ EID_{50}[i] /mL	[60]
Influenza A virus H5N1	Recombinant HA and inactivated virus	50 mM Tris-HCl (pH 7.5), 25 mM NaCl, 5 mM $MgCl_2$, 10 mM DTT[6]	(2) CCGGAATTCCTAATACGACTCGTGTGCATGGATAGCACGTAACGGTGTAGTAGATACGTGCG GGTAGGAAGAAAGGGAAATAGTTGTCCTGTTGTATTGAAAACGCGGCCGCGG (N_{74})	4.65	[56]
Influenza A virus H5N1	polymerase acidic endonuclease domain (PA_N)	20 mM HEPES, 40 mM KCl, 1 mM $MgCl_2$, 1 mM DTT, 1 mM EDTA[h], 10% glycerol	(PAN-1) CCGTAATACGACTCACTATAGGGGAGCTCGGTACCGAATTCTTTAACTTTTTTTTTTTTTT TTTCAATGATAAGCTTTGCAGAGAGGATCCTT	137 ± 21	[42]
			(PAN-2) CCGTAATACGACTCACTATAGGGGAGCTCGGTACCGAATTCGCAAGCGTCTGCATCCC GGTGGGACCATTAAAGCTTTGCAGAGAGGATCCTT	247 ± 11	
			(PAN-3) CCGTAATACGACTCACTATAGGGGAGCTCGGTACCGAATTCTTCATTTTTTTTTTTTTT TCTTTCAGGATAAGCTTTGCAGAGAGGATCCTT	147 ± 23	

			(PAN-4) CCGTAATACGACTCACTATAGGGGAGCTCGGTACCGAATTCAAAGTTCCAATTAAAACG TAGAGTCTTCAGAAGCTTTGCAGAGAGGATCCTT (N_{30})		
Influenza A virus H5N2	Intact virus	100 mM NaCl, 20 mM Tris-HCl (pH 7.6), 2 mM $MgCl_2$, 5 mM KCl, 1 mM $CaCl_2$	(J_3APT) CGTACGGAATTCGCTAGCTGATGGTGTGGCGGGGGGCGGCCTGGGGCGGGCCGCCCGA TGGGATCCGAGCTCCACGTG (JH_4APT) CGTACGGAATTCGCTAGCGGTGGCTCTAGGGCCTATCGTTGCGCCGCGGATCCGAGCT CCACGTG (N_{40})	$6.913 \cdot 10^5 EID_{50}$/mL $8.821 \cdot 10^5$ EID_{50}/mL	[59]
Influenza A virus H5N2	Recombinant HA	20 mM sodium phosphate, 500 mM NaCl, 20 mM imizadole, pH 7.5	(HA12-16) GCUUGACGGAGAUCAAGGGCGAGUCUCA UACCAAGUUGAUGGGG (N_{40})	–	[74]
Influenza A virus H9N2	Intact virus	–	(4D) CCTTGTTCTATTGAACCTCTTAGTCTGGTCCTCA GTTGGG (N_{40})	40.67	[62]
Influenza A virus H9N2	HA	50 mM Tris-HCl (pH 8.3)	(A9) GCTGCAATACTCATGGACAGCCTCCTGGGGTCAGGCTCAGACATTGATAAAGCGACATC GGTCTGGAGTACGACCCTGAA (B4) GCTGCAATACTCATGGACAGGGGCCGCGCCTGGTCGGTTGGGTGGGTGGCGCCCGGGACGGTC TGGAGTACGACCCTGAA (N_{40})	46.2 ± 5.5* 42.5 ± 9.8** 7.4 ± 1.1* 6.4 ± 0.7** *HA; **virus	[89]
Influenza A virus H9N2	Globular region of the recombinant HA	50 mM Tris-HCl (pH 7.4), 5 mM KCl, 100 mM NaCl, 1 mM $MgCl_2$, 100 μg tRNA, 0.2% BSA	(C7) ATTAACCCTCACTAAAGGGAGGTAGTTATAGTATATGGAAGGGGGTGT TATGGTCGAATAAGTTAACG (C7-35 M) GGTAGTTATAGTATATGGAAGGGGGTGTCG TATGG (N_{28})	–	[73]
Influenza B virus	(1) Intact virus (2) Recombinant HA	10 mM HEPES (pH 7.4), 150 mM NaCl, 5 mM $MgCl_2$	(1) GGGAGAAUUCCGACCAGAAGUUUUUGUUUAUAUUGUUGUUUUAUU CCUUUCCUCUCUCCUUCCUCUUCU (2) GGGAGAAUUCCGACCAGAAGGGUCUACGCCCGAAGGGUUGCCGUGCCUUUCCUCUCUCCU UCCUCUUCU (N_{25})	700 ± 200 1200 ± 200	[54]
Influenza B virus	HA	50 mM Tris-HCl (pH 7.5), 25 mM NaCl, 5 mM $MgCl_2$	(A-20) GGGAGCUCAGCCUUCACUGCACUCCGGCUGGUGGACGCGGUACGAGCAAUUUGUACC GGAUGG AUGUUCGGGCAGCGGUGUGGCAGGGAUGAGCGGCACCACGGUCGGAUCCAC (N_{74})	44 ± 6* 28 ± 3** *HA;** virus	[38]
RSV	Inactivated virus	10 μl/mL BSA, 0.1% Tween 20, 0.1 μg/mL poly (dIdC) acid in PBS	(H8) TAGGGAAGAGAAGGACATATGATAGTGCGGTGAGCCGTCGGACATACAAATA CTTGACTAGTACATGACCACTTGA (N_{30})	30 (G protein)	[90]
HPV-16	VLP	PBS	(Sc5-c3) GGGAACAAAAGCUGCACAGGUUACCCCCGCUUGGGUCUCCCUAUAGUG AGUCGUAUUA (N_{15})	$5 \cdot 10^{-5}$	[50]
HBV	Surface antigen	20 mM HEPES (pH 7.35), 120 mM NaCl, 5 mM KCl, 1 mM $CaCl_2$, 1 mM $MgCl_2$	(H01) GGGAATTCGAGCTCGGTACCCACAGCGAACAGCGGCGGACATAATAGTGCTTACTACG ACCTGCAGGCATGCAAGCTTGG (H03) GGGAATTCGAGCTCGGTACCGGCACAAGCATATGGACTCCTCTGAACCTACGATGTAGT ACCTGCAGGCATGCAAGCTTGG (N_{40})	–	[67]
HBV	Surface antigen	20 mM Tris-Cl (pH 8.0), 80 mM potassium acetate, 10% glycerol, 1 mM $MgCl_2$, 0.2 mM EDTA, 10 μM DTT	(HBs-A22) TTAATACGACTCACTATAGTTGATTGCGTG TCAATCATGGCCGTCTATAATGATCGTA AACGACGGGTCATGTGTATGTTGGGGATTGGGACCTGATTGAGTT CAGCCCACATAC (DNA sequence shown although the selection is made for RNA aptamers) (N_{25})	–	[55]
HBV	Recombinant core protein	50 mM NaH_2PO_4, 300 mM NaCl, 10 mM imidazole, pH 8.0	(28) ACGCTCGGATGCCACTACAGCTTCCCCTAATCTGGCGCTCTCATCTAATTTCCCTTCCT GCTCATGGACGTGCTGGTGAC (N_{40})	–	[91]
HBV	e antigen	–	(1) GGGAATTCGAGCTCGGTACCCCAATTCGGGGTGGGCGGCACATCGCGATGCAACGAGC GCTGCAGGCATGCAAGCTTGG (2–19) GGGAATTCGAGCTCGGTACCGGGCGAAGACCGGGACGGGAGGATTCTGTAGATTGG TTTTCTGCAGGCATGCAAGCTTGG (20) GGGAATTCGAGCTCGGTACCGGGCGAGCAACGTAACACTACACGGCGTGTGGGGCTTAA CCTGCAGGCATGCAAGCTTGG (N_{40})	–	[101]
HBV	Recombinant polymerase	0.1 M Sodium phosphate, pH 7.4, 150 mM NaCl, 20 mM imidazole, 0.1% (v/v) NP-40, 100 mg/mL yeast tRNA	(S9) UGUUCAUGUCCUACUGUUCAAACAAAAAAACUGUGCACAAAAAUAAA UUGGGGCAUGGACA (N_{35})	–	[70]
HBV	Recombinant capsid	PBS	(AO-01) GCGGGTCGACGTTTGCACACGCGAGCCGCCATGTCTGGGCCACATCCATGGGCGG (N_{25})	180 ± 82	[92]
HSV-1	Recombinant gD glycoprotein	50 mM Tris-HCl (pH 7.5), 50 mM KCl	(1) GGGAGCUCAGCCUUCACUGCACGAGAGAGGUCGUCCCCAGGGGAGAACUCGUGCUCCUG GAGGCAAGUUGACUGCUCGCUCUCAGCUGGUCAAGGGCACCACGGUCGGAUCCUG	109* 170**	[52]

(*continued on next page*)

Table 2 (*continued*)

Virus	Target	Selection conditions (binding buffer)	Aptamer sequence[a] (5'→3', central region flanked by underlined conserved sequences) (length of the random region of the initial library)	K_D/nM	Reference
			(5) GGGAGCUCAGCCUUCACUGCUAUUAUGAAGUGC GAACUUUAGUCGCGGAAGUGCUGACC AUUGGGCCCAUCCGUGGAGUGGGCACCCCCAGGGGGGCACCACGGUCGGAUCCUG (Mini-1, variant of 1) GGGCACGAGAGAGGUCGUCCCCAGGGGAGAACUCGUGCUCCUGG (N_{74})	39* 40** 32 *native** 2'F–U,C	
VACV	Intact virus	DPBS[j]	(Vac 1) CTCCTCTGACTGTAACCACGCGCGCCCCCGCTGTTCGAGCCGATAGAGGGCTAGTGTCA TGCATAGGTAGTCCAGAAGCC (Vac 2) CTCCTCTGACTGTAACCACGGTCCGTCCTCTCTCGTTTGTTCCTCTTCTCTTATCTGTC AGCATAGGTAGTCCAGAAGCC (Vac 4) CTCCTCTGACTGTAACCACGGATTTCCCAGATCCAATTCAAGTCTCAATATCTACCTC AGCATAGGTAGTCCAGAAGCC (Vac 5) CTCCTCTGACTGTAACCACGCTAGTGCCCCTCTTGTCATCATCTGTTGTTATCTGCCTGG GCATAGGTAGTCCAGAAGCC (Vac 6) CTCCTCTGACTGTAACCACGGTGAGGGTCCTGTGGTTGGTGTGGTTGGTGAGATGTGG TGGGCATAGGTAGTCCAGAAGCC (Vac 14) CTCCTCTGACTGTAACCACGCCATCACCCTA TTATCTCATATCTCGTTTTCCCTATGCGGCATAGGTAGTCCAGAAGCC (Vac 46) CTCCTCTGACT GTAACCACGCGGGATGTAAT ACATTTCAGTGTTGGGACCGTACAGCATAGGTAGTCCAGAAGCC (N_{40})	–	[46]
VACV	Inactivated viral nucleoprotein	Tris buffer (pH 7.3, 0.1% Tween 20), DMEM (0.1% Tween 20) and phosphate buffer (pH 7.5, 0.1% Tween 20)	(A38) TACGACTCACTATAGGGATCCTGTATATA**T**TTTGCA**AC**TAATTGAATTCCCTTTAGTGAGGGTT (non-random nucleotides in bold) (N_{20} random nucleotide positions)	–	[77]

The dash symbol means that the data is not available.

[a] The sequences used in the subsequent tests and/or those of the aptamers with higher affinity are shown. (5'→3', central region flanked by underlined conserved sequences, and length of the random region of the initial library when provided).

[b] Phosphate buffered saline.

[c] Polysorbate 20.

[d] Tris (hydroxymethyl)aminomethane.

[e] Dithiothreitol.

[f] Bovine serum albumin.

[g] Ethylenediaminetetraacetic acid.

[h] 4-(2-Hydroxyethyl)-1-piperazine ethanesulfonic acid.

[i] Median embryo infectious dose.

[j] Dulbecco's phosphate buffered saline.

selectivity of the aptamers [41]. The success of SELEX heavily relies on the efficiency of the separation step after interaction (see below), and to facilitate this separation different tags have been incorporated to the protein or protein fragment such as Histidine (His) or glutathione S-transferase (GST) tags. Non-structural proteins that are crucial for virus replication, as is the case of polymerase acidic (PA) for *influenza A virus* [42], NS5B RNA replicase [24] for HCV, integrase [33,43] or reverse transcriptase [44,45] for HIV-1 and EBOV protein 24 [34] have also been employed. All this information is summarized in Table 2, where it is highlighted how several aptamers have been selected for the same virus using different targets, giving rise to different sequences and affinity characteristics. The properties of the aptamers obtained, in terms of affinity and selectivity, can be influenced not only by the type of target but also by the selection process, thus demonstrating its ability to lead to a wide range of affinity reagents based on genetically encoded sequences with high binding affinities.

A purified single target is not always required, and intact virus (active or inactive) can also be used as target (Table 2). The selection can even be targeted to a whole cell (Cell-SELEX), previously infected with the virus [46], a method very useful for providing the native state protein. A variant consists of performing the selection with target cells that express a viral protein on their surface (CS-SELEX) [47,48].

In cases where viruses are not easily propagated in tissue culture, as it is the case of *noroviruses* (NoV), it is possible to use virus-like particles (VLPs) as targets for selecting aptamers [49]. VLPs are the result of a self-assembling process of structural viral proteins. They mimic viruses but are non-infectious because they lack the viral genetic material, being excellent vaccine candidates. For example, the *papillomavirus* (HPV) vaccine is based on this principle, and HPV Type 16 VLPs have been used for selecting aptamers against this virus [37,50].

2.3. Separation method

The aptamer selection process requires a procedure to separate the oligonucleotides bound to the target from the unbound. An ideal separation technique must be practical (i.e. simple and rapid) and ensure a complete separation, without disturbing the aptamer-target complex. As mentioned above, this is one of the critical steps in the selection process. There is a plethora of separation methods that are routinely used, which can be classified in two groups: i) solution-phase methods based on the homogeneous interaction between the library and the target in solution, followed by the separation and, ii) solid-phase methods, based on the immobilization of the target on a solid support and a heterogeneous target-aptamer pool interaction.

The first SELEX approaches were performed using solution-phase methods in combination with membranes that retain the aptamer-target complexes and allow unbound aptamers to pass through. This approach is widely used in the selection of antiviral aptamers, most commonly with membranes of nitrocellulose [23,27,30,33,38,43–45,51–56], or mixed cellulose esters [47,57], but polyvinylidene fluoride membranes have also proven effective [50]. To remove nonspecific membrane binders, negative selections must be performed by passing the pool through the membrane in the absence of the target before the positive selection against the target. Although the target does not need to be modified, in general a high number of cycles are required to achieve significant enrichment.

A higher rate of enrichment, thus reducing the number of rounds required, can be achieved by selecting a more efficient separation method. Capillary electrophoresis (CE) allows the separation between the bound and unbound sequences on the basis of differences in their electrophoretic mobility once the interaction took place in solution. However, the small sample volume limits the variability of the library. CE-SELEX has been reported for the selection of aptamers specific to the H9N2 subtype of *influenza A virus* [58] and the EBOV protein 24 (eVP24) [34] with affinities in the nanomolar range and only four and six cycles, respectively.

Another SELEX variant that does not require immobilization of the target is GO-SELEX, where graphene oxide (GO) is used as separation support taking advantage of its ability to adsorb ssDNA through π-π stacking but not the ssDNA-target complex. RNA aptamers cannot be selected by this approach. In this way, DNA aptamers for whole avian *influenza virus* particles of H5N2 subtype [59] were developed. To obtain aptamers with broader specificity able to recognize H5Nx whole viruses, different virus subtypes (H5N1, H5N2, and H5N8) were combined as targets in a multi-GO-SELEX approach [60].

The use of solid-phase methods has led to efficient separations, which are combined with stringent washing steps for reducing non-specific binding. Different solid-phase supports have been employed ranging from microtiter plates [48,61–64] to micro- or nanoparticles. The particulate solid phases can be divided in two types, magnetic and non-magnetic.

Magnetic beads (MB) are commonly employed because they facilitate the separation and washing steps, simply by applying a magnetic field, avoiding the use of centrifugation systems. This variant of SELEX is called MB-SELEX. To immobilize intact viruses or VLPs, the particles are previously coated with a specific antibody against the target, which is then immobilized by the affinity interaction [49,65]. In the case of proteins, they can be covalently bound to particles modified with carboxylic groups [66,67] or bound through affinity interactions, for which a prior modification of the proteins is necessary. Thus, streptavidin-modified MB have been used for biotin-labeled target binding [24,37]. For recombinant proteins, a six-histidine tag (His-tag) is often introduced which is then used for their immobilization on Ni-NTA-coated magnetic particles [42,68,69]. The ease of handling of the magnetic support has made possible the automation of the entire SELEX process by a microfluidic SELEX chip, which integrates different modules for the aptamer incubation, magnetic-based separation and nucleic acid amplification by PCR [65].

Non-magnetic particle matrices include agarose beads that have high binding capacities. They are coated with glutathione [39] or the complex between Ni ions and the chelating ligand nitrilotriacetic acid (NTA) [31,70,71] for the immobilization of recombinant proteins containing glutathione S-transferase (GST) or histidine tags, respectively. These beads are also useful as stationary phases for separation under flow conditions in affinity chromatography [41,72–76]. A careful control of the elution of the aptamers bound to the target is required, in such a way that it is even possible to perform the selection in only one interaction step. This is achieved by using a gradient salt elution and collecting the last fractions, where the high affinity binding species will be eluted [62]. Another variant of SELEX that is performed in a single affinity chromatographic step is MonoLEX. In this case, after the interaction between the immobilized target and the library inside the column, the affinity resin is physically segmented to recover the aptamer-families with the highest affinity toward the target, which are amplified by PCR [77].

In general, the SELEX variants discussed so far require multiple selection cycles for transforming the starting library in a pool of nucleic acids with high affinity to the target. After every few selection cycles, an off-line evaluation of the average affinity of the pool is required to ensure that the selection is evolving properly. In SPR-SELEX, the target is immobilized on the chip of a surface plasmon resonance (SPR) spectrometry instrument, where the

interaction step takes place, providing real-time information of the enrichment process [22,25].

Positive rounds of selection, incubating the library with the target, must always be combined with negative or counter-selection steps to remove from the successive pools the sequences that show non-specific binding. Negative selections are made by incubating the nucleic acids' collection with all the components used for the interaction/separation step except the target molecule, such as membranes or filters, spheres, or nanoparticles. Counter-selections involve the incubation of the library with a negative control target, such as uninfected cells in the Cell-SELEX or those that do not express the virus protein in the CS- SELEX, [54,67,75,77]. These selections are performed before each round of positive selection [53,54,65], or after certain number of them [60]. Transfer RNA (tRNA) is also often added as a non-specific binder competitor. Counter-selections are particularly important to obtain aptamers able to distinguish between very similar viruses or virus subtypes [39,61].

To ensure the specificity and affinity of the selected aptamers, the stringency of the interaction must be gradually increased through the successive selection cycles. This is achieved by modifying the library: target ratio, the concentration of the competitor or the interaction time [38,52]. With this aim, the incubation time between the library and the target is usually decreased; the library: target ratio is increased by reducing the target amount while keeping constant the library [23,30,69]. It is also common to increase the number of washing steps during the separation process [23] or the amount of the competitor (tRNA). In general, the change in the interaction conditions for the different rounds is very empirical and no general rule or protocol can be established.

2.4. Amplification and conditioning steps

The oligonucleotide sequences displaying affinity toward the target must be amplified and conditioned in order to obtain a new pool of single-stranded nucleic acids to initiate a new cycle of selection. The protocol differs depending on whether DNA or RNA aptamers are being developed. RNA pools are amplified by reverse transcription polymerase chain reaction (RT-PCR), which combines reverse transcription of the RNA sequences to amplifiable cDNA and PCR. The dsDNA copies are then usually purified by phenol–chloroform extraction and subsequently transcribed back to RNA. At the end of the transcription reaction, the DNA templates must be digested with DNase I and the remaining RNA transcripts purified by denaturing polyacrylamide gel [23,51]. To preserve the abundance of the original library, it is important to optimize the number of PCR cycles, avoiding the amplification of a skewed population in the pool [52].

In the case of DNA aptamers, the amplification is directly performed by PCR, although amplification of such a heterogeneous mixture of templates is not easy, and the formation of PCR by-products or PCR parasites may introduce some bias during this step [78]. For this reason, it is recommended to determine the optimal PCR amplification cycles, confirming the successful amplification of fragments of the expected size [66]. Next a conditioning step is required in order to generate ssDNA from the corresponding dsDNA. Different methods are available for this purpose: asymmetric PCR, unequal strand length PCR, biotin-streptavidin separation and lambda exonuclease digestion [10].

Asymmetric PCR is a rapid and straightforward approach, used in the generation of aptamers against *influenza* [63], *hepatitis B virus*, HBV [67] and HCV [57]. It is based on using an unequal molar ratio of forward and reverse primers during the amplification, with an excess of the forward one, to preferentially amplify the sense strand. The extreme situation is to use only the forward primer for amplification [57]. The main drawback of this approach is its low efficiency, which can lead to a significant loss of sequence information.

Another possibility for preferentially amplifying one of the strands is to design one of the primers with a stem-loop structure, which is termed unequal strand length PCR. This was the strategy followed to obtain aptamers against the *influenza virus*, subtype H1N1 [61]. In this case, one of the primers was elongated to contain a 5′-GC rich sequence with the ability to form a stem-loop structure with a high melting temperature. This structure remains folded during the DNA polymerase reaction, thus preventing the elongation of the corresponding strand. The purification of the amplicons by denaturing-gel electrophoresis results in two bands, the lower one corresponds to the desired single strand template. More efficient than the previous one, this approach requires a careful design of the primers.

The most widely used strategy involves the modification of one of the PCR primers (the reverse one) with biotin at its 5' terminus. After the amplification, the double-stranded amplicons are entrapped onto streptavidin-modified beads, either agarose or most commonly magnetic beads, by the affinity interaction between biotin and streptavidin. The non-biotinylated strand is then eluted after alkaline denaturing the attached dsDNA. This was the approach followed for the selection of aptamers recognizing human NoV [49], HIV-1 [44,45], SARS CoV-2 [79], EBOV [66], and different subtypes of *influenza virus* [42,75,76]. The possible loss of streptavidin during the NaOH treatment, which could act as an additional target, is one of the main limitations of this method.

The modification of one of the primers with a terminal 5′-phosphate group is used in combination with the treatment of the amplicons with an exodeoxyribonuclease, lambda exonuclease, which preferentially cleaves the phosphorylated strand in the obtained amplicons. In this way, high quality ssDNA is obtained in an efficient process. A final purification step for removing the exonuclease is required before starting the following cycle, which lengthens the process. This was the method chosen to obtain aptamers against *Zika virus*, ZIKV [69], EBOV [34], *severe fever with thrombocytopenia syndrome virus*, SFTSV [64] and *influenza virus* [39,56].

The PCR amplification steps are the most expensive and time-consuming in the SELEX process. A non-SELEX approach for the selection of aptamers has been developed, which involves successive partitioning steps without PCR amplification between them [80,81]. This method is simple, reduces the time required for selection, and can be more easily automated. Although originally conceived in combination with non-equilibrium capillary electrophoresis for separation [81], it has been recently combined with partitioning steps involving particulate solid phases with the immobilized target [82]. Selective aptamers for the influenza A virus, subtype H1N1 have been obtained in this way. The starting library was incubated simultaneously with two types of particles, which contained two close targets (proteins characteristic for H1N1 and H3N2 subtypes); the competition of the library for the two targets during the repetitive steps of partitioning led to an enrichment in specific binders over the non-specific ones. This process called SELCOS, Systemic Enrichment of Ligands by COmpetitive Selection, could be especially useful to easily obtain aptamers capable of discriminating very similar targets.

2.5. Post-SELEX modifications

Once aptamers have been identified through the SELEX process, it is common to optimize them to improve their affinity and *in vivo* stability or just to reduce the cost of synthesis. Among the different strategies described for this post-SELEX modification [83], anti-

viral aptamers have been mainly optimized by truncation, chemical modification and mutagenesis.

The ideal aptamer length for commercial applications is in the range 20–40 nucleotide residues, and in order to obtain the minimal sequence for binding, aptamers are usually truncated in an empirical way. It is accepted that the binding of the aptamers to their cognate targets is associated with the formation of a functional secondary structure, which does not normally involve the constant regions (primer binding regions) [84]. Consequently, in many cases the truncation process begins by eliminating these regions at both ends [48,57,62,68,74]. However, in some cases a small part of the primer binding region has been found to be involved in binding [73]. For this reason, it is recommended to carry out the truncation in a rational way, by analyzing the secondary structure using bioinformatic tools. There are different computer simulation programs, such as Mfold [85] or ValFold [86], to predict the most stable structure based on thermodynamic considerations. Hairpin loops [71] and G-quadruplex structures [68,75] are often found as part of the recognition by antiviral aptamers, and the deletion of nucleotides that are not involved in these structures does not affect [31] or even improve the affinity [52]. The study of the binding site by empirical [52,71] or computational methods, such as molecular docking and molecular dynamic simulations [79] efficiently guide the truncation process.

Chemical modification is aimed to improve the *in vivo* stability, increasing the resistance against nucleases, for example by replacing all the pyrimidine nucleotides with 2′-fluoro derivatives [52]. Additionally, to improve the therapeutic potential it is necessary to increase the pharmacokinetic lifetime, which is achieved by adding polyethylene glycol (PEG) to one end of the aptamer and conjugating it to a macromolecule such as cholesterol [29].

Finally, site-directed mutagenesis can be used to identify the binding motif of the aptamer [23]. This is a laborious process, which was performed on a second generation of aptamers against the HIV-1 aspartyl protease, showing how the substitution of some of the nucleotides increases the affinity of the aptamers, while replacement of others prevents their binding.

3. Aptasensors and aptamer-based assays for virus detection

The availability of aptamers to specifically recognize different viruses opens the door to new sensitive, rapid and low-cost diagnostic methods, mainly through their integration into biosensors. A biosensor is an analytical device consisting of a bioreceptor and a transducer. The first one is aimed to specifically recognize a target analyte. The second converts the energy of the binding between the bioreceptor and the analyte into a measurable signal. This signal is related to the concentration of the analyte in the sample, ideally with minimal sample treatment. Biosensors can be optical, piezoelectric or electrochemical depending on the type of transducer they contain. If aptamers are used as bioreceptors, the biosensors are called aptasensors.

The aptasensor designs most used in viral detection are next analyzed. These designs can be broadly classified into two categories: direct and sandwich sensors. The direct format is the simplest one; it is based on the trapping of the viral particles or proteins derived from the virus by the aptamers onto the transducer surface, which leads to a change in the output signal without the use of additional markers. In the sandwich format assay, two aptamers are required to bind simultaneously to the analyte: i) the capture receptor, which is immobilized on the transducer and selectively entraps the virus, and ii) the signaling aptamer that acts as an indicator system, leading to the transducer signal to reveal the presence of the virus. With this aim, the signaling aptamer can incorporate different types of markers, depending on how the final transduction process is performed. In some cases, a mixed sandwich design is chosen in which an aptamer is combined with another type of receptor, most commonly an antibody, although others such as lectins have also been used.

Table 3 compiles the different aptamer-based assays and aptasensors described so far, classified according to the virus detected; it summarizes the target, the type of transduction and the aptamer used in each case, tracing each aptamer to the original work mentioned in Table 2, where the selection process is described. Note that the aptamer sequences are those indicated with the same nomenclature in Table 2. Table 3 also includes the achieved limits of detection (LOD) and the response time, when provided.

3.1. Optical aptamer-based assays

Optical transduction, based on monitoring the changes taking place after the interaction of light with the sample, are the most commonly used in combination with aptamers for virus detection. About 60% of the aptamer-based viral diagnostic applications evaluated are based on this type of transduction, 50% are assays for the detection of *influenza viruses*.

Aptamers are considered chemical antibodies and the most straightforward approach is to incorporate them into assays analogous to enzyme-linked immunosorbent assays (ELISA). These tests are used for detecting viral proteins or whole viruses in microtiter plates following a sandwich format. The surface of the plastic wells is coated with a binder of the virus-specific protein, the capture receptor, either an aptamer or an antibody. Thereafter, the sample is incubated and the virus or the viral protein is entrapped onto the wells. The affinity complex is then detected by adding a labeled receptor (aptamer or antibody), which binds to a different epitope of the viral protein and allows the direct or indirect incorporation of an enzyme as reporter molecule. When the two receptors are aptamers the assay is termed enzyme-linked aptamer sorbent assay (ELASA), also known as enzyme-linked oligonucleotide assay (ELONA). Different combinations of capture and signaling binders have been used: aptamer-aptamer [62,75] (Fig. 2A), antibody-aptamer [47,64] (Fig. 2B) and aptamer-antibody [28,69] (Fig. 2C). The optimal configuration depends on the affinity and the selectivity of the available receptors.

Aptamers can be immobilized onto the wells by adsorption of amine-modified oligonucleotides onto activated surfaces [69,75], by affinity interaction using biotinylated oligonucleotides onto streptavidin-coated plates [62] or through the hybridization reaction, elongating the aptamer with oligo $(dA)_{16}$ and using biotin-oligo $(dT)_{16}$-streptavidin-modified wells [28]. Most commonly the signaling aptamer is modified with biotin, requiring an additional incubation step with a streptavidin-enzyme conjugate before performing the optical transduction [36,47,64,69,75]. The use of streptavidin-peroxidase conjugate in combination with hydrogen peroxide and tetramethylbenzidine [36,64,69,75] or *o*-phenylendiamine [47] allows the colorimetric detection of viral proteins with a LOD in the ng/mL range as demonstrated for ZIKV detection with a LOD of 100 ng/mL [69]. The quantification of infectious HCV particles has also been reported with a similar strategy, resulting in a method that has proven useful for monitoring the efficacy of anti-HCV drugs [36]. The sensitivity of the assay strongly depends on the affinity of the signaling binder. The LOD of the above assay for ZIKV is improved by three orders of magnitude by pairing the same capture aptamer with a monoclonal antibody with higher affinity than the selected signaling aptamer toward the target protein. It is also possible to decrease the LOD by increasing the number of enzymes incorporated per recognition event (Fig. 2B). This approach is achieved using liposomes encapsulated with

peroxidase and coated with replication protein A (RPA) as a reporter system [64]. RPA specifically recognizes the ssDNA in the affinity complex on the wells, without affecting the large-aptamer binding. Thereafter, the lysis of the liposomes releases the enzymes, whose activity is measured by colorimetry with TMB as a substrate. In this way, the sensitive detection of the SFTSV nucleocapsid protein has been reported, with a LOD of 9 pg/mL, improving the detectability by more than one order of magnitude when compared to the use of streptavidin-peroxidase conjugate (LOD 0.12 ng/mL).

In ELASA the analyte concentration is inferred by measuring the activity of the enzyme coupled to the entrapped affinity complex. For this purpose, a substrate of the enzyme is added, and the amount of product enzymatically generated is measured after a fixed time. The most commonly used enzymes are peroxidase (like in the previous examples) and alkaline phosphatase. Substrates of these enzymes can be selected that give rise to chemiluminescent products with inherently better sensitivity. Thus, the combination of an aptamer against the nucleocapsid protein of SARS-CoV with an ALP-labeled antibody, using a chemiluminescence transduction process, led to the detection of N protein at a concentration as low as 20 pg/mL [28].

Fluorescence can also be used as read-out technique, combined with receptors directly linked to a fluorescent molecule. This strategy has been explored for HCV detection by exploiting protein-chip technology [40]. The authors combined an RNA aptamer against the core antigen of HCV and an antibody conjugated to the cyanine dye Cy3. However, the detectability was poor, which may be due to the lack of amplification provided by the enzyme in the abovementioned approaches.

A relevant advantage of using aptamers as signaling receptors is that they can be directly coupled to real-time PCR, simply elongating the signaling aptamer with a DNA fragment acting as a primer in the PCR process. This is a sensitive and a highly reproducible approach that allowed the detection of only 100 $TCID_{50}$/mL of H9N2 *influenza A viruses* [62] ($TCID_{50}$ is the fifty-percent-tissue culture-infective dose, a unit usually employed to measure the infectious virus titer). This test can be directly used with swab samples without passing by an extraction step of viral genome, demonstrating its usefulness in clinical samples.

The optical aptamer-based assays hitherto described require multiple separation and washing steps, which can be simplified by using magnetic beads as supports to link the capture receptor. These solid supports have been combined with schemes similar to previously mentioned ELASAs for the detection of different viruses. Using an aptamer-antibody pair, Xi et al. [67] described the chemiluminescence detection of HBV surface antigen (HBsAg) with a linear range of 1–200 ng/mL and a LOD of 0.1 ng/mL in serum samples, improving the performance of the ELISA test commonly used for the detection of HBV infection [67]. Magnetic beads have also been covalently linked to aptamers against the globular region of HA to detect *influenza A* H3N2 *virus* [93]. In this work, the interaction between concanavalin A (ConA) and the protein glycans is used to obtain the sandwich complex. ConA is a lectin that specifically binds α-D-mannosyl and α-D-glucosyl residues and it can be easily conjugated to glucose oxidase (GOx). The biocatalytic cycle of GOx is then linked to the growth of gold nanoparticles to obtain colored solutions in the presence of the H3N2 virus, reporting a LOD of 11.16 μg/mL.

A great advantage of magnetic beads is their ease of manipulation, allowing their integration into microfluidic systems for automation of the assays [66,94]. An aptamer able to recognize different types and subtypes of *influenza virus* has been immobilized onto magnetic beads for virus entrapment and combined with the same aptamer but conjugated to fluorescein for fluorescent detection. By exploiting the conformational changes of this aptamer when exposed to different ion concentrations, it is possible to simultaneously detect three *influenza viruses*: *influenza A* H1N1, H3N2, and *influenza B*, with a LOD of 3.2 HAU (hemagglutination units) in only 20 min [94]. The automation is especially useful for the detection of high-risk viruses like EBOV, improving the biosafety of the assays. Thus, a magnetically-controlled detection chip based on the use of aptamers specific for GP EBOV protein linked to magnetic nanospheres and the same biotin-labeled aptamers, allowed the development of a sandwich assay for detecting the virus in the concentration range of 5.0–150.0 ng/mL, with a LOD of 4.2 ng/mL. A fluorescence signal is obtained after incubation with a streptavidin-quantum dot conjugate, which is directly acquired in the chip via a fiber optical spectrometer [66].

Although ELISA-type tests are the most well-established method for aptamer-based optical detection of virus, these are laboratory-based assays that require multi-step protocols for complex sample processing and specialized instrumentation. Exploiting the unique optical properties of gold nanoparticles (AuNPs), direct assays based on aptamers have been developed for visual detection of *Dengue virus*, DENV [95] and *flu virus* [96], which provide potential advantages for their use in decentralized environments. These assays rely on the modification of AuNPs with the aptamers, the subsequent interaction with the corresponding target led to a change in the solution color, mainly associated to the aggregation of AuNP. While simple, these assays are characterized by a rather poor sensitivity (detection of 3×10^8 viral particles for *flu virus*) [96].

Lateral flow assays (LFA) based on antibody recognition have been used in resource-limited settings for decades, and it is not surprising that they have also been coupled to aptamers to achieve devices that combine the benefits of both. A scheme of the two approaches used in LFA, sandwich and competitive formats, is displayed in Fig. 3. The sandwich format is used for detecting whole viruses, which are captured between two different aptamers (Fig. 3A) [59] or by pairing an aptamer with an antibody (Fig. 3B) [97]. In both cases, *influenza viruses* are detected using AuNPs as detection particles, conjugated to the signaling aptamer or the antibody, respectively. The biotinylated-capture aptamer can be located in the test line forming a complex with streptavidin [59]. Alternatively, it can be added to the sample to favor its interaction with the virus in solution and subsequently captured in the test line, which is modified with streptavidin [97]. In the control line, it is possible to use a DNA probe, which hybridizes with the signaling aptamer [59] or an antibody recognizing the detection antibody modified with AuNP [97]. In both cases, the positive result is seen when the two lines (test and control) become colored. The competitive assay (Fig. 3C) is intended for detecting circulating viral proteins instead of the whole virus. It has been reported for the detection of HCV core antigen [98]. In this case, the test and control lines are modified with two DNA probes partially complementary to the recognition aptamer, which is conjugated to AuNPs. In the example, the test line contains a complex between streptavidin and a biotinylated-antisense aptamer (DNA probe 1), whereas the control line is modified with streptavidin-biodin-dT_{21} (DNA probe 2). The DNA probe 1 competes with HCV core Ag for combining with the aptamer, in such a way that if the analyte is present it binds with the aptamer, which is subsequently unable to bind at the test line. A lack of color at the test line is therefore indicative of a positive result. The aptamer is elongated with polyA, and will always hybridize in the control line, indicating that the test runs as expected. Although this kind of tests are easily performed, they give qualitative or semi-quantitative results, with limited sensitivity.

It is also possible to take advantage of the high sensitivity of fluorescence spectrometry to develop highly sensitive detection tests, where the whole assay is performed in a tube within a relatively short time (typically 30 min). These assays are especially suitable for point-of-care (POC) diagnostic. They require the use of fluorescence species, which can be linked to the aptamers in two ways: by intercalation or by covalent binding. In the first case, the fluorescence of the molecule in solution is quenched by water molecules, but after intercalation in a double-strand structure, an enhancement of fluorescence occurs due to the hydrophobic environment between the base pairs. This is the approach reported for detecting recombinant hemagglutinin (rHA) protein of the H5N1 *influenza virus* in human serum [99]. Thiazole orange (TO) is used as a reporter molecule in combination with a selective aptamer; the presence of rHA protein in solution induces a quadruplex secondary structure in the aptamer to form the affinity complex, where TO intercalates with the subsequent fluorescence emission. The aptamer is conjugated to the surface of Ag@SiO2 nanoparticles, which act as a metal-enhanced fluorescence (MEF) system amplifying even more the response and leading to a LOD of 3.5 ng/mL in human serum.

Inspired by the molecular beacon approach, the use of a fluorophore-quencher system makes possible the design of homogeneous assays where the aptamer-target binding also induces a change in fluorescence from an OFF to an ON state. As a proof of concept, Yamamoto and Kumar were the first to apply this approach for the detection of the HIV Tat protein using an RNA aptamer [100]. They split an anti-Tat aptamer into two oligonucleotides, one being designed to form a hairpin structure and modified with a fluorophore (fluorescein) and a quencher (DABSYL) at both ends (Fig. 4A). In this state, the fluorophore and quencher are in close proximity, resulting in low fluorescence (OFF state). Aptamer-target interaction opens the hairpin, to form a ternary complex in the presence of the second part of the whole aptamer. This process shifts the fluorophore far from the quencher, with a subsequent increase in fluorescence (ON state). If the aptamer has not a hairpin structure, a similar effect can be achieved by designing a DNA sequence partially complementary to the aptamer and covalently linked to the quencher. The hybridization between both sequences leads to quenching. The same pair fluorescein-DABSYL was chosen for detecting HBeAg for HBV diagnosis [101]. When deployed in serum samples, the presence of the protein led to the complex aptamer-protein with the subsequent release of DNA-quencher, restoring the fluorescence (Fig. 4B). This allowed the detection of only 609 ng/mL (26.5 nM) of HBeAg in 2 min. Quenching can also be achieved by interaction of the fluorescein-labeled aptamer with multiwall carbon nanotubes (MWCNT) or graphene oxide (GO) (Fig. 4C). The quantification of NoV was thus successfully performed, leading to a lower LOD when using GO, probably because its greatest efficiency as quencher [102]. Quantum dots (QDs) have also been used as fluorescent labels, allowing superior performance due to their particular photophysical properties, in combination with Iowa black as dark quencher [103,104]. When combined with a three-dimensional photonic crystal, a highly sensitive and selective test for the quantitative analysis of *influenza A* H1N1 *virus* has been reported, adapted to the use of a smartphone camera for resource-limited settings [103].

The energy transfer from an excited fluorescent molecule (the donor) to an acceptor molecule is exploited in a fluorescence excitation transfer (FRET)-based competitive aptaassay for the detection of HBV surface antigen (HBsAg) [105]. The principle of this assay is shown in Fig. 4E. The FRET donor (Cy3) is coupled to the aptamer, whereas the acceptor (Cy5) is linked to HBsAg. The formation of the aptamer-HBsAg complex brings the two fluorophores close, and the fluorescence of the donor is reduced. When free sample HBsAg is present in the reaction mixture it will compete for the aptamer with the labeled-HBsAg, and the fluorescence of the donor increases. This is a one-step assay, with no requirements of sample pretreatment, achieving a sensitivity 40-fold higher than a chemiluminescence immunoassay commonly used in clinical applications, and similar selectivity.

Intra chemiluminescent resonance transfer (Intra-CRET) is another alternative for developing cost-effective and simple aptamer-based assays. In this approach, a fluorescein-modified aptamer is linked to a tail of 5 guanines, which react with 3,4,5-trimethoxylphenylglyoxal (TMPG) to give an excited intermediate that directly transfers energy to fluorescein emitting chemiluminescence. The interaction with the virus targeted by the aptamer quenches the emission. This made possible the quantification of NoV GII capsids in tap water above 80 ng/mL without sample treatment [106].

Although the above aptamer-based assays offer new opportunities for viral detection, they cannot be considered true aptasensors, since they do not integrate recognition and transduction. To simplify the protocol and avoid the introduction of optical labels, aptamers are immobilized on the surface of label-free transduction systems like surface plasmon resonance (SPR). The changes in the refractive index of the sensing layer as a result of its interaction with the virus are directly monitored and related to the viral load in the sample. Using a portable SPR system avian *influenza virus* H5N1 has been detected in poultry swab samples in 1.5 h in the concentration range 0.128−1.28 HAU, with excellent selectivity against other non-target virus subtypes [107]. The sensitivity is improved using a second aptamer functionalized with AuNPs [60], being able to detect the whole virus in H5N1-infected feces samples, although the advantage of a label-free approach is lost. New instrumental developments, such as localized surface plasmon resonance [108] or surface plasmon fluorescence spectroscopy [54] could further improve detectability. However, they are in their infancy and so far, only shown as a proof of concept. Something similar happens with Surface-enhanced Raman scattering (SERS), under intense investigation in recent years due to its speed and great sensitivity. Only a proof of concept has been developed for the detection of the *influenza virus*, resulting in a non-quantitative test with poor reproducibility that also requires labels for optimal sensitivity [109].

3.2. Electrochemical aptasensors

Electrochemical sensors, where the chemical energy of the selective interaction between the recognition element and the target is directly transduced into an electrical signal (current, potential or impedance), require simple and low-cost instrumentation and are easy to miniaturize and integrate into automatic systems without compromising their analytical characteristics. This makes them especially suitable devices for POC testing, to be used close to the patient, outside the facilities or clinical laboratories, for a rapid diagnostic. Despite their potential and versatility, aptamer-based electrochemical sensors have been less explored, representing 32% of the devices evaluated in Table 3, of which, again, more than 50% correspond to applications for *influenza viruses*' detection.

The semiconductor electronic device called field effect transistor (FET) is the basis for the development of label-free aptasensors, where measurements are performed under equilibrium conditions. This device is formed of a series of semiconductor-insulator-metal layers (Fig. 5A), with three terminals: source (S), drain (D) and gate (G). Between S and D there is an active channel, which conductivity depends on the potential (V_G) applied between G and S; charge carriers flow from the source to the drain (drain current, I_D) through the channel, modulated by V_G. This standard configuration

is modified by covalently immobilizing an aptamer on the gate (Fig. 5B) [110] or on the active channel between source and drain (Fig. 5C) [111–113], in such a way that the specific binding of the target protein results in a shift of the drain current-gate voltage that is correlated with the protein concentration (Fig. 5D). There are two different approaches for measurement: i) the response is determined by a change in the threshold voltage (V_T) defined as the gate voltage needed to maintain a certain drain current, ii) the change in the drain current at a constant gate voltage is used as a response (Fig. 5). The conventional FET, using silica as semiconductor have been used [110], but nanomaterial-based semiconductors such as carbon nanotubes [112] and multidimensional conductive nanofilm composed of vertically oriented carboxylic polypyrrole nanowires and graphene layer [111] are also investigated. The main advantage of these devices is that they can be adapted to mass production using microelectronic technology, offering great sensitivity and selectivity. Aptamer-based FET have been developed to detect HA protein, biomarker of *influenza virus*, in chicken serum samples within a dynamic range of 10 pM to 10 nM and a LOD of 5.9 pM [110] and the HIV-Tat protein at 600 pM level [112]. Sensing by means of FET devices can be improved by a smart design of the nanomaterial place in the active channel, being able to detect as low as 10 aM of HBsAg in human serum and artificial saliva, with great potential for the noninvasive real-time diagnosis of hepatitis B [111].

Electrochemical impedance spectroscopy (EIS) provides the principle of another type of label-free sensing approaches. The aptamer-target interaction involves the formation of multiple non-covalent bonds between both species, which produces a change in the solvated ion concentration within the sensing layer when this interaction takes place on the surface of a working electrode. As a consequence, a change in the local conductivity occurs, which can be monitored by means of non-faradaic impedance measurements [114,115]. The electrical change in the sensing layer can also be monitored using faradaic impedance spectroscopy in the presence of a redox probe in solution [46,61,68,116].

Non-faradaic impedance is used in microfluidic chips that houses an interdigitated microelectrode array, where specific aptamers are immobilized. The microelectrodes can be fabricated from gold [115] or a conductive polymer [114]. The recognition of the virus by the aptamers is indicated by an increase in the impedance, likely caused by the blockage of the flow of ions between the microelectrode fingers. A notable advantage of these platforms is speed, the detection of 10^3 PFU of H1N1 *influenza A virus* has been reported in less than 15 min without any additional reagents [114].

Faradaic impedance in the presence of ferricyanide/ferrocyanide ions as redox probe has been used to detect or quantify *influenza A* [61,68], HCV [116] and *vaccinia virus*, VACV [46]. The aptamer is immobilized onto the working electrode, which constitutes the selective layer, and the recognition process results in a change in the electron-transfer resistance, R_{et}, a measurement of the rate of the electron transfer between the redox probe and the electrode. R_{et} is very sensitive to the state of the sensing layer, but it is not possible to predict how it will change as a consequence of the recognition process. Depending on the nature of the working electrode, the density of the immobilized aptamer on the electrode surface or the physical properties of the analyte, the recognition process can lead to an increase or a decrease in R_{et}. For example, the immobilization of an aptamer able to selectively recognize viable VACV onto gold microelectrodes by hybridization of the aptamer with a chemisorbed ssDNA, led to a decrease of R_{et} after recognition [46]. This was attributed to the conformational change of the aptamer induced by its binding to the target, which alters the structure of the sensing phase making the redox probe more accessible to the conductive surface. A similar effect was observed by immobilizing an anti-influenza A aptamer by chemisorption on gold electrodes [61]. In this work, the effect of the aptamer surface density is demonstrated, obtaining 100 times higher sensitivity for the high-density probe sensors (~1×10^{12} aptamers/cm^2), with a LOD of 0.9 pg/μL, 300 times better than the obtained with an ELASA using the same aptamer. The opposite trend, an increase in R_{et} after target binding, is observed when an anti-HCV core antigen was immobilized by adsorption onto glassy carbon electrodes modified with graphene-quantum dots composites [116]. This effect was associated to the blocking access of the redox probe to the surface by the recognized protein.

Although these label-free aptasensors have demonstrated high sensitivity and selectivity, the faradaic impedance measurement requires recording the whole impedance spectrum over a wide range of frequencies. This typically takes at least 10 min per measurement, a period of time in which the sensing layer can spontaneously reorganize, giving rise to poor reproducibility. This problem has been partially addressed by using differential pulse voltammetry (DPV) or cyclic voltammetry (CV) instead of EIS during the measurement step, making possible the selective detection of H1N1 subtype of *influenza A virus* on indium-tin oxide surfaces where aptamer was immobilized by adsorption [68] or covalently [117]. Interestingly, in the first case the peak current of the redox probe decreases as the virus concentration increases [68], whereas in the second one the signal increases with the concentration of HA protein used as biomarker [117]. As the measurement principle is the same as in the impedimetric sensors, this difference can be interpreted in terms of the nature of the target (the whole virus in one case and a protein in the other) and aptamer packing density, probably higher when the aptamer is physically adsorbed. The ability of nanomaterials to increase the active sensing surface and minimize the electrode surface fouling renders their use very advantageous for improving the response characteristics of this type of sensor. Thus, the use of nanocomposites of multiwalled carbon nanotubes and chitosan [118], or porous graphene oxide and molybdenum sulfide [119], allowed the sensitive detection in serum samples of the HCV core antigen and the L1-major capsid protein of *human papilloma virus*, respectively.

The oligonucleotide nature of aptamers can be exploited to design multifunctional probes, which incorporates a sequence responsible for the electrochemical signal. This is the case of the *influenza A virus* aptasensor constructed on a porous AuNPs-modified gold electrode [120]. An anti-HA aptamer is a fragment of the immobilized probe that also includes a DNAzyme mimicking peroxidase activity. The DNAzyme forms a complex with hemin, and the Fe^{3+}/Fe^{2+} redox center of hemin gives a characteristic peak that is monitored by CV. The binding of HA to the aptamer part hampers the electron transfer process of the hemin, leading to a decrease in the peak current measured by CV, which is correlated with the amount of the target protein above 1 pM in diluted-chicken serum.

Although enzyme labels allow very sensitive aptasensors to be designed as a consequence of the large amount of detectable product is obtained from a single molecule, they have been scarcely used in the design of electrochemical aptasensors for the detection of viral targets. Interestingly, only one aptasensor with a sandwich assay format and amperometric detection has been described, using this principle. Diba et al. [121] constructed an aptasensor to detect the HA protein of the H5N1 virus in diluted human serum, by modifying a carbon electrode with gold nanoparticles covered with the specific aptamer. A monoclonal antibody conjugated to alkaline phosphatase binds to the target, completing the sandwich. The transduction was carried out using as a substrate of the enzyme 4-

Table 3
Applications of aptamers in the diagnostics of viral infections.

Virus	Target	Transducer (detection method)	Format assay	Aptamer[a]	Limit of detection (assay time)	Reference
Human NoV	Intact virus	Optic (chemiluminescence, Intra-CRET)	Direct	SMV-25 [49] (only the central region and the sequence GGGGGTTTT at the 5′ end)	80 ng/mL	[106]
Human NoV	Intact virus	Optic (fluorescence quenching with CNT or GO)	Direct	SMV-21 [49]	4.4 ng/mL (CNT) 3.3 ng/mL (GO)	[93]
HCV	Intact virus	Optic (colorimetric, ELASA)	Sandwich	ZE2 [47]	–	[47]
HCV	Intact virus	Optic (colorimetric, ELASA)	Sandwich	E2-A, E2-B, E2-C and E2-D [36]	$1.25–2.50 \cdot 10^3$ FFU[b]/mL monovalent $3.13–6.25 \cdot 10^2$ FFU/mL multivalent	[36]
HCV	Capsid antigen	Optic (visual detection, lateral flow)	Direct	9-15 [40] (only with the central region), DNA aptamer	100 pg/mL by the naked eye or 10 pg/mL using a scanner (10 min)	[98]
HCV	Capsid antigen	Optic (fluorescence)	Sandwich	9-15 [40], RNA aptamer	–	[40]
HCV	Capsid antigen	Electrochemical (EIS)	Direct	ACTATACACAAAAATAACACGACCGACGAAAAAACACAACC [116]	1.67 fg/mL	[116]
HCV	Capsid antigen	Electrochemical (EIS)	Direct	ACTATACACAAAAATAACACGACCGACGAAAAAACACAACC [116]	3.3 pg/mL	[118]
ZIKV	NS1 protein	Optic (colorimetric, ELASA)	Sandwich	2 and 10 [69]	100 ng/mL in buffer	[69]
DENV	Intact virus	Optic (colorimetric magnetic particles)	Direct	S15 [72], only the central region elongated with 3 C at the 5′ and 3 G at 3′ ends	–	[95]
HIV-1	Tat protein	Optic (fluorescence)	Sandwich	CGCGAAGCUUGAUCCCGAGAGCUUC and CUCGGUCGAUCG CUUC (derived from ACGAAGCUUGAUCCCGUUUGCCGGUCG AUCGCUUCGA [100])	–	[100]
HIV-1	Tat protein	Piezoelectric (QCM)	Direct	ACGAAGCUUGAUCCCGUUUGCCGGUCGAUCGCUUCGA [100]	0.65 ppm 0.25 ppm (heat-treated aptamer)	[125]
HIV-1	Tat protein	Electrochemical (FET)	Sandwich	UCGGUCGAUCGCUUCAUAA and GAAGCUUGAUCCCGAA [100]	1 nM	[113]
HIV-1	Tat protein	Electrochemical (FET)	Sandwich	UCGGUCGAUCGCUUCAUAA and GAAGCUUGAUCCCGAA [100]	600 pM	[112]
SARSCoV	Nucleocapsid protein	Optic (chemiluminescence, microplates)	Sandwich	1 [28]	20 pg/mL (~8 h)	[28]
EBOV	Intact virus	Optic (magnetismcontrolled chip)	Sandwich	GP-D01 and NP-C04 [66]	4.2 ng/mL antiglycoprotein aptamer	[66]
SFTSV	Nucleocapsid protein	Optic (colorimetric, microplates)	Sandwich	SFTS-apt 3 [64]	0.009 ng/mL	[64]
Influenza A H1	HA	Electrochemical	Direct	ApI [39], also for H5 detection	nM range	[117]
Influenza A H1N1	Intact virus	Optic (fluorescence, microfluidic system)	Direct	Antisense sequence of the aptamer [65]. Also used for H3N2 and *influenza B virus* detection	3.2. HAU (20 min)	[94]
Influenza A H1N1	Intact virus	Optic (fluorescence)	Direct	RHA0006 [75]	Buffer: 70 ng/mL; 138 pg/mL (portable) (20 min) Serum: 550 ng/mL; 600 ng/mL (portable)	[103]
Influenza A H1N1	Intact virus	Electrochemical (non-faradaic impedance)	Direct	A22 [41]	10^3 PFU[c]/mL (less than 15 min)	[114]
Influenza A H1N1	Intact virus	Electrochemical (CV and EIS)	Direct	V46 [68]	3.7 PFU/mL	[68]
Influenza A H1N1	Inactivated virus	Electrochemical (EIS)	Direct	A20S (only the central region) [61]	0.9 pg/μL	[61]
Influenza A H3N2	Intact virus	Optic (lateral flow)	Sandwich	P30-10-16 [53]	$2 \cdot 10^6$ virus (~15 min)	[97]

(*continued on next page*)

Table 3 (*continued*)

Virus	Target	Transducer (detection method)	Format assay	Aptamer[a]	Limit of detection (assay time)	Reference
Influenza A H3N2	Intact virus	Optic (colorimetric, magnetic beads)	Sandwich	A22 [41]	11.16 μg/mL	[93]
Influenza A H3N2	Intact virus	Optic (sedimentation and visual detection)	Direct	P30-10-16 [53] for H3N2 and A-20 [38] for *influenza B virus* detection	$3 \cdot 10^8$ virus (more than 10 min)	[96]
Influenza A H3N2	Intact virus	Optic (SERS)	Direct	RHA0385 [75]	$1 \cdot 10^{-4}$ HAU[d]/sample $2 \cdot 10^4$ virus/sample	[109]
Influenza A H5N1	Intact virus	Optic (SPR)	Direct	2 [56] (only the central region)	0.128 HAU (1.5 h)	[107]
Influenza A H5N1	Intact virus	Optic (SPR)	Direct	IF22 and IF10 [60]	200 EID_{50}[e]/mL	[60]
Influenza A H5N1	Intact virus	Optic (fluorescence)	Sandwich	2 [56] (only the central region)	0.4 HAU (30 min)	[104]
Influenza A H5N1	Intact virus	Piezoelectric (QCM)	Direct	2 [56] (only the central region)	2^{-4} HAU/50 μL, 0.0128 HAU (30 min)	[123,124]
Influenza A H5N1	Intact virus	Electrochemical (impedance)	Direct	2 [56] (only the central region)	0.0128 HAU (30 min)	[115]
Influenza A H5N1	Intact virus	Electrochemical (enzyme nanogate)	Direct	2 [56] (only the central region)	2^{-9} HAU (1 h)	[122]
Influenza A H5N1	HA	Optic (colorimetric, ELASA)	Sandwich	RHA0006, RHA0385 [75]	0.1 μg/well	[75]
Influenza A H5N1	HA	Optic (fluorescence, MEF)	Direct	TTGGGGGCGGGAGGGTTTATTGGGGTT	2–3.5 ng/mL (less than 30 min)	[99]
Influenza A H5N1	HA	Optic (SPR)	Direct	2 [56], only with the central region and modified with a tail (TTGCCATGTGTATGTGGG) at the 3′ end	1 pM in PBS or diluted chicken serum	[108]
Influenza A H5N1	HA	Electrochemical (enzyme reaction)	Sandwich	RHA0385 [75]	100 fM	[121]
Influenza A H5N1	HA	Electrochemical (CV, hemin)	Direct	2 [56], only with the central region and modified with a tail (TTGCCATGTGTATGTGGG) at the 3′ end	1 pM in HEPES or diluted chicken serum	[120]
Influenza A H5N1	HA	Electrochemical (FET)	Direct	2 [56], only with the central region and modified with a tail (TTGCCATGTGTATGTGGG) at the 3′ end	5.8 pM in buffer and 5.9 pM in real samples	[110]
Influenza A H5N2	Intact virus	Optic (lateral flow)	Sandwich	J_3APT and JH_4APT [59]	Buffer: $6 \cdot 10^5$ (eye); $1.27 \cdot 10^5$ EID_{50}/mL (software) Duck feces: $1.2 \cdot 10^6$ (eye); $2.09 \cdot 10^5$ EID_{50}/mL (software)	[59]
Influenza A H9N2	Intact virus	Optic (real time PCR)	Sandwich	4D [62]	100 $TCID_{50}$[f]/mL	[62]
Influenza B	Intact virus	Optic (SPFS)	Direct	1 [54]	ng/mL range	[54]
HPV-16	L1 protein	Electrochemical	Direct	Sc5-c3 [50]	0.1 ng/mL (1.75 pM)	[110]
HBV	Surface antigen	Optic (FRET)	Direct	HBs-A22 [55], antisense DNA sequence	12.5 pmol/mL	[96]
HBV	Surface antigen	Optic (chemiluminescence)	Sandwich	H01 [67]	0.1 ng/mL	[67]
HBV	Surface antigen	Electrochemical (FET)	Direct	H03 [67]	10 aM	[111]
HBV	E antigen	Optic (fluorescence)	Direct	1, 2–19 and 20 [92]	609 ng/mL (2 min)	[101]
VACV	Intact virus	Electrochemical (EIS)	Direct	Vac 1, Vac 2, Vac 4, Vac 5, Vac 6, Vac 14 and Vac 46 [46]	330 PFU or ~60 virus/mL (more than 1 h)	[46]

The dash symbol means that the data is not available.

[a] Aptamer name as included in Table 2 or its sequence (5 '→ 3′) if not. [Information about the reference where it is described].

[b] Focus forming units.

[c] Plaque forming units.

[d] Hemagglutination units.

[e] Median embryo infectious dose.

[f] Median tissue culture infectious dose.

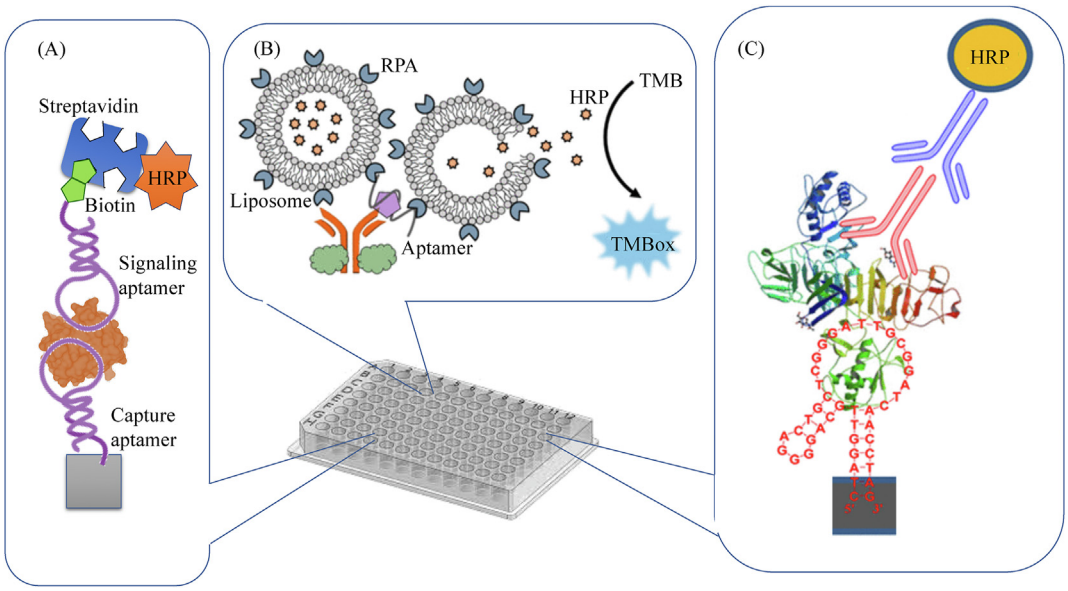

Fig. 2. Optical aptamer-based assays performed onto microtiter plates. (A) Two aptamers are used as capture and signaling binders, with streptavidin-horseradish peroxidase (HRP) conjugate as a reporter. (B) Antibody-aptamer pairing, using HRP-encapsulated liposomes for signal enhancement (adapted with permission from Ref. [64]). (C) Aptamer is used for capturing and peroxidase-labeled antibody as signaling receptor (adapted with permission from Ref. [69]).

aminophenylphosphate, which is enzymatically hydrolyzed to 4-aminophenol, amperometrically detected.

An innovative and very interesting approach makes use of the bionanogate principle for the selective detection of H5N1 subtype of *avian influenza A virus* over other subtypes such as H1N1, H2N2, H4N8 and H7N2, which can be easily adapted for detecting other viruses [122]. The sensor is constructed onto a glassy carbon electrode coated with a cross-linked layer of lactate dehydrogenase and bovine serum albumin. A nanoporous gold film is then attached on the electrode, where a pair of ssDNA probes are chemisorbed. The probes are designed to hybridized with an aptamer recognizing the HA protein of the virus, in such a way that the linked aptamer restricts the access of substrates of the enzyme through the nanopore so the nanogate is in the closed state. In the presence of the virus, the complex aptamer-virus is formed, and the aptamer is released form the surface, triggering the nanogate to an open state. The enzyme activity behind the nanogate is electrochemically monitored and quantitatively related with the virus titer in solution in the range 2^{-10} to 2^{2} HAU. Although it shows great sensitivity, this approach has not yet been demonstrated in the context of real samples and it is not easily adapted to mass-production.

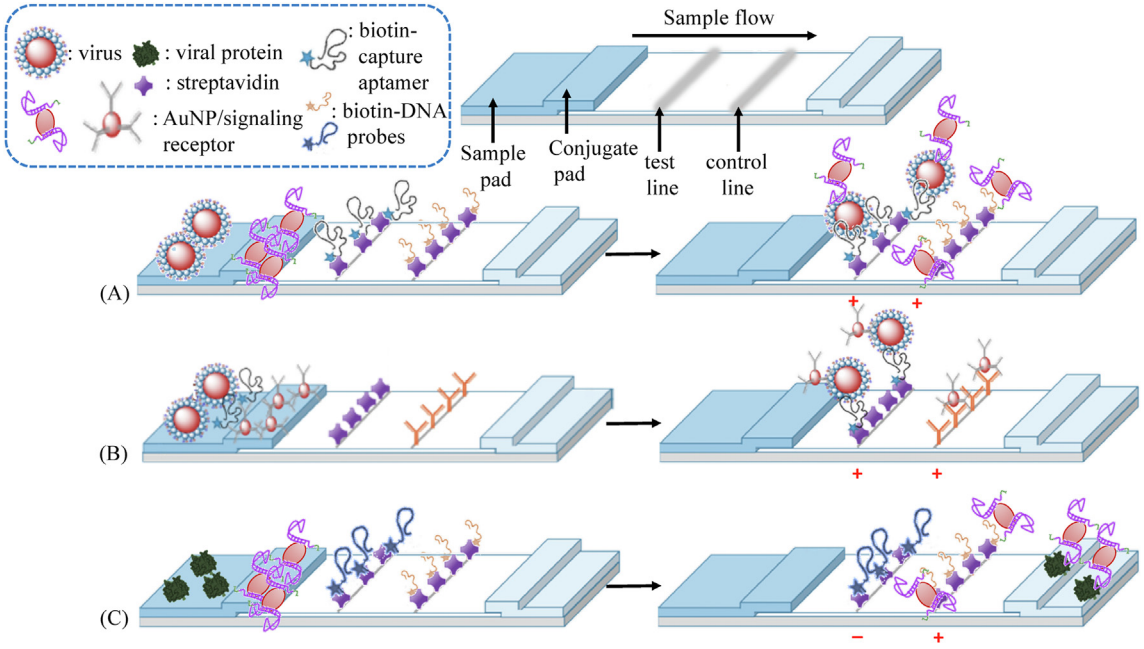

Fig. 3. Scheme of lateral flow assays for virus detection. (A) Sandwich format using two aptamers as capture and signaling receptors. (B) Sandwich format with a capture aptamer and a signaling aptamer (adapted with permission from Ref. [97]). (C) Competitive format, with two DNA probes partially complementary to the signaling aptamer. The first one competes with the viral protein for binding to the aptamer. The signaling receptor is labeled with gold nanoparticles for visualization.

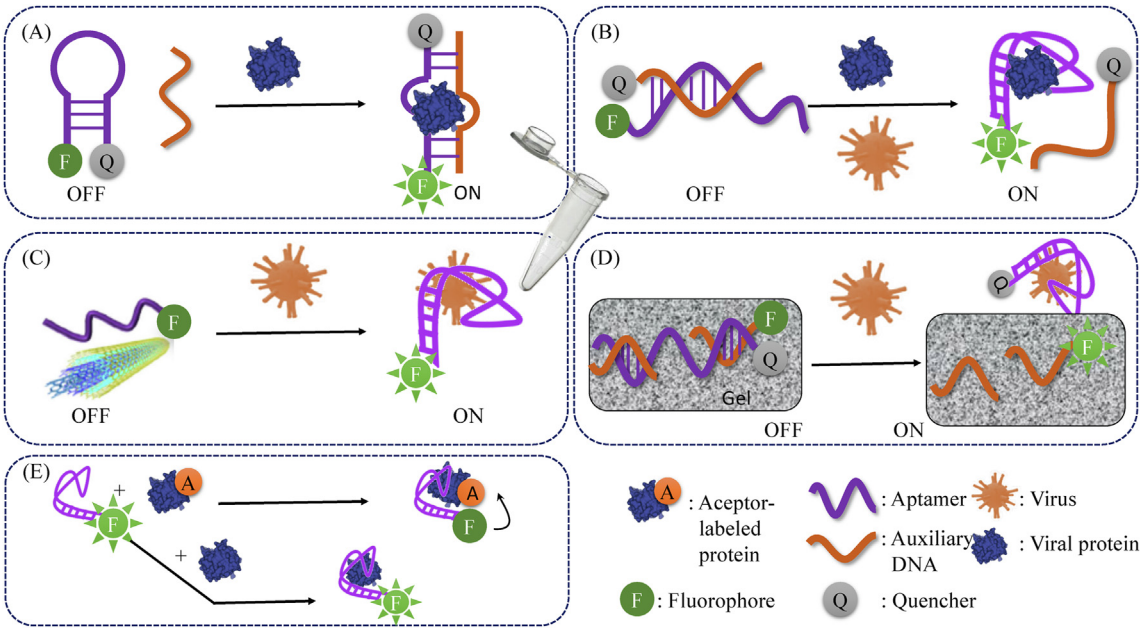

Fig. 4. Schemes for the different homogeneous aptamer-based assays with fluorescence transduction for virus detection. (A) Fluorophore and quencher are attached to the aptamer (molecular beacon) (adapted with permission from Ref. [100]). (B) The fluorophore-linked aptamer is quenched after hybridization with a sequence labeled with the quencher. (C) MWCNT are used as a quencher (adapted with permission from Ref. [102]). (D) The aptamer modified with a quencher is attached to a hydrogel by hybridization to a short DNA.A second auxiliary DNA modified with a QD is also included in the gel, quenched because of the close proximity to the aptamer (adapted with permission from Ref. [104]). The virus-aptamer interaction caused the recovery of the fluorescence of the label in all cases. (E) Competitive assay based on FRET, using an aptamer modified with the donor and the target modified with the acceptor.

3.3. Piezoelectric aptasensors

Quartz crystals that have piezoelectric properties are the starting material to build this type of sensor. When a weight is placed on a quartz crystal, a certain charge density appears on its surface, the magnitude of which is proportional to the weight deposited. The effect is reversible, so that, if an oscillating electrical field is applied between the two faces of a quartz crystal, it vibrates. Each crystal has its own resonance frequency, and this is altered when small masses are deposited on it. The quartz crystal microbalance (QCM) takes advantage of this effect. It consists of a thin quartz disk with two gold electrodes deposited on both sides of the crystal, between

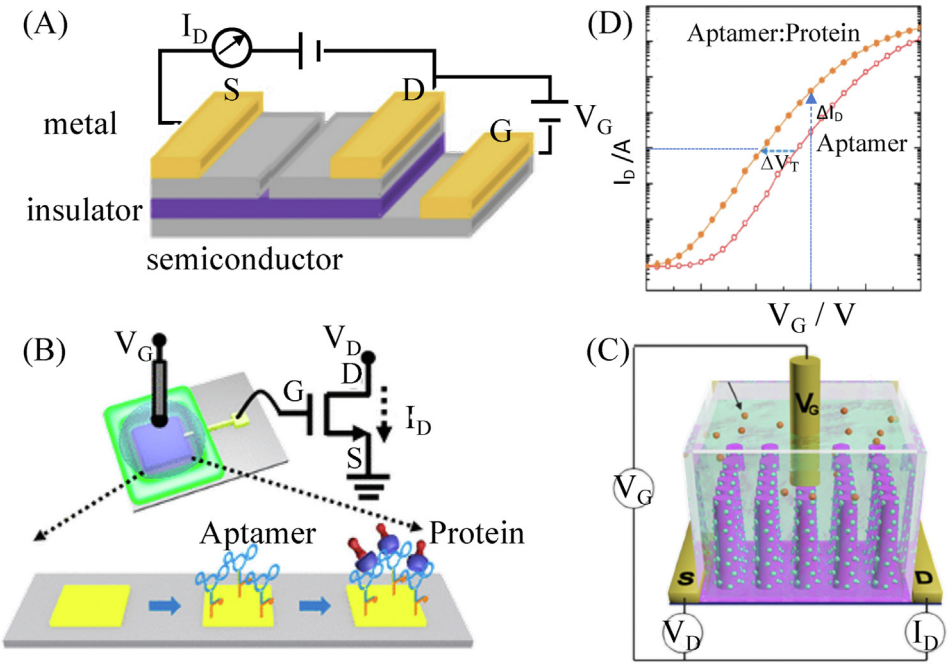

Fig. 5. Aptamer-based field effect transistor (FET). (A) Structure and wiring of a FET, which is transformed in an aptasensor by immobilizing an aptamer onto (B) the gate, G or (C) on the channel between the source, S and the drain, D. (D) The interaction aptamer-protein results in a shift in the characteristic drain current, I_D-gate voltage, V_G, using as response either the change in I_D at a constant V_G or the displacement in the threshold potential (V_T) needed to maintain a certain I_D.

which an alternating potential difference is applied. This excitation induces oscillations of the crystal under resonance conditions. By depositing a mass on this structure, there is a change in the resonance frequency of the crystal, measured by a frequency detector. When an aptamer is immobilized on one of the electrodes and it captures its cognate target, the formation of the aptamer-target complex leads to changes on the surface that result in a decrease in the resonance frequency. Label-free QCM aptasensors for the detection of *influenza A* H5N1 *virus* [123,124], and the Tat protein of HIV-1 [125] have been reported. The immobilization of the aptamer on the gold surface of QCM was carried out by creating a self-assembled monolayer of 16-mercaptohexadecanoic acid where the aptamer is then covalently bound through an amide bond [123], or by coating the electrode with streptavidin and labeling the aptamer with biotin [125]. It is important to note that the QCM responds nonspecifically to any change in mass, so the selectivity of the sensor depends solely on the selectivity of the aptamer used to capture the analyte. Additionally, the immobilization of the aptamer should avoid non-specific interactions at the sensing layer and ensure good stability. The aptamer density on the surface also affects the sensitivity achieved. Thus, the modification of the QCM chip with a gold nanowell structure effectively increased the immobilization capacity of aptamers, which resulted in improved sensitivity, being able to detect 2^{-4} (0.062) HAU in chicken tracheal swab samples in 10 min [123]. QCM responds to changes not only in mass but also in viscosity occurring on the sensing surface. This is the reason why when the same aptamer was immobilized onto the QCM sensor synthesizing a poly (acrylamide-co-aptamer) hydrogel the LOD lowers to 0.0128 HAU. The binding of virus led to a change in the hydrogel from a shrink to swelling state, which results in a change of viscosity and consequently an increased sensitivity [124]. The analytical performance appears competitive with similar immunosensor approaches and could be further improved by post-recognition amplification, a possibility that has not been explored so far.

4. Conclusions and perspectives

Since the first aptamer for the recognition of a human infective virus was described in 2000, substantial progress in the selection of anti-viral aptamers has been accomplished, and these affinity-based molecules are becoming an alternative to antibodies in the biotechnology scene for the diagnosis of viral infections. Although aptamers are functionally comparable to antibodies, they have many potential advantages. (1) They have a small size (5–25 kDa) and a flexible structure, which improves their ability to penetrate tissues and allows their efficient entry into cells and their compartments. (2) They are made by quick chemical synthesis in a simple and reproducible process, which leads to high purity formulations, minimizing batch-to-batch variations. (3) They can be stored at room temperature without degrading and can be subjected to versatile chemical modification for improving their properties. (4) They do not induce immune responses, nor do they have toxicity.

Despite the abovementioned advantages, aptamers have not yet fully demonstrated their potential for improved antiviral therapeutics and detection. One important reason is that there is not a standard protocol for the selection of aptamers that could be applied to any type of target, and the conditions of selection have to be adapted to each specific case. In addition, the published aptamers are in general poorly characterized, which makes very difficult to compare the selection strategies or sequences selected against the same virus but using different targets. For example, the nucleotide sequences of the published aptamers are not always easily found, nor the selection conditions or their affinity characteristics. When the sequence is provided, it is not always clear if the randomized central region or the whole aptamer (including the constant flanking regions) were used for characterization. Some RNA aptamers are provided as DNA sequences, which is confusing since it is known that an RNA aptamer cannot be transferred to DNA maintaining its characteristics. In order to avoid these pitfalls, we suggest that all information regarding the selection process should be detailed and rigorous guidelines for aptamer characterization must be stablished.

A barrier that limits the practical applications of aptamers is that they have to be used in conditions similar to those used during their selection. It is desirable to select conditions that lead to aptamers that exhibit both high affinity and high selectivity. However, this is not easy to achieve using conventional SELEX, as conditions are generally sought to enrich by affinity (positive selection) or by specificity (negative selection), but rarely both are simultaneously achieved. Although it is generally stated that aptamers have better stability than antibodies, it should be noted that their stability in biological media is quite limited, due to the presence of nucleases, especially RNA aptamers. This is of particular concern in therapeutic applications, and is one of the reasons why the use of DNA aptamers is preferred in diagnostic applications.

The current limitations offer new opportunities to stablish recommendations for future work which will greatly help to keep up with viral emergence. One opportunity is to streamline the selection process, preferably using selection conditions close to the natural media in which the viruses must be detected or treated so as not to compromise their subsequent application. The use of high-throughput sequencing has becoming more frequent, thus making possible the identification of high-affinity aptamers in a lower number of selection cycles. In this context, the development of new bioinformatics tools could contribute to improve the aptamer selection. Similarly, the development of miniaturized automatic platforms is an attractive approach for reducing the reagent consumption and the time required to complete the aptamer selection, making it more cost-effective.

This review comprehensively collects the sequence information on anti-viral aptamers that may have diagnostic or therapeutic utility. Besides, this information could be a valuable resource for facing the remarkable mutation capacity of viruses. These sequences could be the starting point for obtaining second-generation aptamers selected from partially randomized pools to display enhanced affinities and specificity towards the mutant virus.

Regarding virus detection, this review illustrates the great variety of aptasensors developed with this aim. This clearly indicates that aptamers are excellent tools for rapid diagnosis of emerging pathogens, with potential for shortening the times from diagnosis to treatment. The fastest aptamer-based diagnostic methods reported so far have response times ranging from 2 to 30 min. Optical and electrochemical methods are widely used to transduce the virus recognition by aptamers. Most of them require labeling either for immobilization or detection, which demands a complete knowledge of the secondary structure of the aptamer and the binding sites to the target. Label-free approaches like FET and impedance measurements or SPR are particularly useful to develop disposable biosensors suitable to be integrated in point-of-care devices. Exciting opportunities exist in combining aptamers with nanomaterials to improve their immobilization in the sensing layer and as advanced labels, both in optical and electrochemical transduction. Another unrealized potential is to take advantage of the nucleic acid nature of aptamers to combine them with novel isothermal nucleic acid amplification strategies like rolling circle amplification (RCA) or terminal deoxynucleotidyl transferase (TdT). Using these approaches, the development of extremely sensitive

diagnostic tools may be envisaged. A lack of uniformity has been detected when reporting on the LOD of the developed devices, which makes extremely difficult to compare them in terms of sensitivity. It would be recommended to stablish common criteria that also allow their comparison with the methods currently used. The ultimately value of these devices is their clinical utility. However, only a limited number of the described strategies has been shown to support the virus detection in authentic clinical samples (saliva, urine, serum samples). Compatibility with a wide range of samples must be stablished for aptamer-based diagnostic tests to become useful in clinical settings. For their ultimate success and utility, some important issues should also be resolved, with an emphasis on their simplification, portability, and the feasibility of large-scale manufacturing.

In summary, the development of antiviral aptamers holds great promise, simplifying the development of specific receptors for virus and lowering their development cost. With continued developments in diagnosis applications, they could help to change the way by which virus infections are diagnosed. Intensive interdisciplinary research efforts are needed in this area to address the challenges of diagnosis of viral infections to be better prepared for the next global pandemic.

Declaration of competing interest

The authors declare that they have no known competing financial interests or personal relationships that could have appeared to influence the work reported in this paper.

Acknowledgements

This work was supported by the Spanish Ministerio de Ciencia y Universidades (RTI-2018-095756-B-I00), the municipality of Ribera de Arriba/La Ribera (Asturias, Spain) and Principado de Asturias Government (IDI2018-000217), co-financed by FEDER funds.

References

[1] K.E. Jones, N.G. Patel, M.A. Levy, A. Storeygard, D. Balk, J.L. Gittleman, P. Daszak, Global trends in emerging infectious diseases, Nature 451 (2008) 990–993. https://doi.org/10.1038/nature06536.
[2] M. Woolhouse, F. Scott, Z. Hudson, R. Howey, M. Chase-Topping, Human viruses: discovery and emergence, Phil. Trans. R. Soc. B. 367 (2012) 2864–2871. https://doi.org/10.1098/rstb.2011.0354.
[3] W.I. Lipkin, S.J. Anthony, Virus hunting, Virology 479–480 (2015) 194–199. https://doi.org/10.1016/j.virol.2015.02.006.
[4] X. Zou, J. Wu, J. Gu, L. Shen, L. Mao, Application of aptamers in virus detection and antiviral therapy, Front. Microbiol. 10 (2019) 1462. https://doi.org/10.3389/fmicb.2019.01462.
[5] S. Afrasiabi, M. Pourhajibagher, R. Raoofian, M. Tabarzad, A. Bahador, Therapeutic applications of nucleic acid aptamers in microbial infections, J. Biomed. Sci. 27 (2020) 6. https://doi.org/10.1186/s12929-019-0611-0.
[6] A. Díaz-Fernández, R. Lorenzo-Gómez, R. Miranda-Castro, N. de-los-Santos-Álvarez, M.J. Lobo-Castañón, Electrochemical aptasensors for cancer diagnosis in biological fluids – a review, Anal. Chim. Acta 1124 (2020) 1–19. https://doi.org/10.1016/j.aca.2020.04.022.
[7] V. González, M. Martín, G. Fernández, A. García-Sacristán, Use of aptamers as diagnostics tools and antiviral agents for human viruses, Pharmaceuticals 9 (2016) 78. https://doi.org/10.3390/ph9040078.
[8] B. Kudłak, M. Wieczerzak, Aptamer based tools for environmental and therapeutic monitoring: a review of developments, applications, future perspectives, Crit. Rev. Environ. Sci. Technol. 50 (2020) 816–867. https://doi.org/10.1080/10643389.2019.1634457.
[9] P. Kumar, Monitoring intact viruses using aptamers, Biosensors 6 (2016) 40. https://doi.org/10.3390/bios6030040.
[10] T.K. Sharma, J.G. Bruno, A. Dhiman, ABCs of DNA aptamer and related assay development, Biotechnol. Adv. 35 (2017) 275–301.
[11] C.H. van den Kieboom, S.L. van der Beek, T. Mészáros, R.E. Gyurcsányi, G. Ferwerda, M.I. de Jonge, Aptasensors for viral diagnostics, Trends Anal. Chem. 74 (2015) 58–67. https://doi.org/10.1016/j.trac.2015.05.012.
[12] T. Wang, C. Chen, L.M. Larcher, R.A. Barrero, R.N. Veedu, Three decades of nucleic acid aptamer technologies: lessons learned, progress and opportunities on aptamer development, Biotechnol. Adv. 37 (2019) 28–50. https://doi.org/10.1016/j.biotechadv.2018.11.001.
[13] Y. Zhang, B. Lai, M. Juhas, Recent advances in aptamer discovery and applications, Molecules 24 (2019) 941. https://doi.org/10.3390/molecules24050941.
[14] W. Zhou, P.-J. Jimmy Huang, J. Ding, J. Liu, Aptamer-based biosensors for biomedical diagnostics, Analyst 139 (2014) 2627–2640. https://doi.org/10.1039/c4an00132j.
[15] D. Ellington, J.W. Szostak, *In vitro* selection of RNA molecules that bind specific ligands, Nature 346 (1990) 818–822. https://doi.org/10.1038/346818a0.
[16] C. Tuerk, L. Gold, Systematic evolution of ligands by exponential enrichment: RNA ligands to bacteriophage T4 DNA polymerase, Science 249 (1990) 505–510. https://doi.org/10.1126/science.2200121.
[17] A.D. Ellington, J.W. Szostak, Selection *in vitro* of single-stranded DNA molecules that fold into specific ligand-binding structures, Nature 355 (1992) 850–852. https://doi.org/10.1038/355850a0.
[18] C. Tuerk, S. MacDougal, L. Gold, RNA pseudoknots that inhibit human immunodeficiency virus type 1 reverse transcriptase, Proc. Natl. Acad. Sci. U.S.A. 89 (1992) 6988–6992. https://doi.org/10.1073/pnas.89.15.6988.
[19] W. Pan, R.C. Craven, Q. Qiu, C.B. Wilson, J.W. Wills, S. Golovine, J.F. Wang, Isolation of virus-neutralizing RNAs from a large pool of random sequences, Proc. Natl. Acad. Sci. Unit. States Am. 92 (1995) 11509–11513. https://doi.org/10.1073/pnas.92.25.11509.
[20] J. Wang, H. Jiang, F. Liu, *In vitro* selection of novel RNA ligands that bind human cytomegalovirus and block viral infection, RNA 6 (2000) 571–583. https://doi.org/10.1017/S1355838200992215.
[21] R. Stoltenburg, C. Reinemann, B. Strehlitz, SELEX—a (r)evolutionary method to generate high-affinity nucleic acid ligands, Biomol. Eng. 24 (2007) 381–403. https://doi.org/10.1016/j.bioeng.2007.06.001.
[22] T.S. Misono, P.K.R. Kumar, Selection of RNA aptamers against human influenza virus hemagglutinin using surface plasmon resonance, Anal. Biochem. 342 (2005) 312–317. https://doi.org/10.1016/j.ab.2005.04.013.
[23] S. Duclair, A. Gautam, A. Ellington, V.R. Prasad, High-affinity RNA aptamers against the HIV-1 protease inhibit both *in vitro* protease activity and late events of viral replication, Mol. Ther. Nucleic Acids 4 (2015) e228. https://doi.org/10.1038/mtna.2015.1.
[24] A. Biroccio, J. Hamm, I. Incitti, R. De Francesco, L. Tomei, Selection of RNA aptamers that are specific and high-affinity ligands of the hepatitis C virus RNA-dependent RNA polymerase, J. Virol. 76 (2002) 3688–3696. https://doi.org/10.1128/JVI.76.8.3688-3696.2002.
[25] M. Khati, M. Schuman, J. Ibrahim, Q. Sattentau, S. Gordon, W. James, Neutralization of infectivity of diverse R5 clinical isolates of human immunodeficiency virus type 1 by gp120-binding 2JF-RNA aptamers, J. Virol. 77 (2003) 12692–12698.
[26] G.M. London, B.M. Mayosi, M. Khati, Isolation and characterization of 2′-F-RNA aptamers against whole HIV-1 subtype C envelope pseudovirus, Biochem. Biophys. Res. Commun. 456 (2015) 428–433. https://doi.org/10.1016/j.bbrc.2014.11.101.
[27] J. Zhou, P. Swiderski, H. Li, J. Zhang, C.P. Neff, R. Akkina, J.J. Rossi, Selection, characterization and application of new RNA HIV gp 120 aptamers for facile delivery of Dicer substrate siRNAs into HIV infected cells, Nucleic Acids Res. 37 (2009) 3094–3109. https://doi.org/10.1093/nar/gkp185.
[28] D.-G. Ahn, I.-J. Jeon, J.D. Kim, M.-S. Song, S.-R. Han, S.-W. Lee, H. Jung, J.-W. Oh, RNA aptamer-based sensitive detection of SARS coronavirus nucleocapsid protein, Analyst 134 (2009) 1896–1901. https://doi.org/10.1039/b906788d.
[29] C.H. Lee, Y.J. Lee, J.H. Kim, J.H. Lim, J.-H. Kim, W. Han, S.-H. Lee, G.-J. Noh, S.-W. Lee, Inhibition of hepatitis C virus (HCV) replication by specific RNA aptamers against HCV NS5B RNA replicase, J. Virol. 87 (2013) 7064–7074. https://doi.org/10.1128/JVI.00405-13.
[30] S. Shubham, J. Hoinka, S. Banerjee, E. Swanson, J.A. Dillard, N.J. Lennemann, T.M. Przytycka, W. Maury, M. Nilsen-Hamilton, A 2′FY-RNA motif defines an aptamer for ebolavirus secreted protein, Sci. Rep. 8 (2018) 12373. https://doi.org/10.1038/s41598-018-30590-8.
[31] S.R. Han, S.-W. Lee, Inhibition of Japanese encephalitis virus (JEV) replication by specific RNA aptamer against JEV methyltransferase, Biochem. Biophys. Res. Commun. 483 (2017) 687–693. https://doi.org/10.1016/j.bbrc.2016.12.081.
[32] I. Alves Ferreira-Bravo, C. Cozens, P. Holliger, J.J. DeStefano, Selection of 2′-deoxy-2′-fluoroarabinonucleotide (FANA) aptamers that bind HIV-1 reverse transcriptase with picomolar affinity, Nucleic Acids Res. 43 (2015) 9587–9599. https://doi.org/10.1093/nar/gkv1057.
[33] K.M. Rose, I. Alves Ferreira-Bravo, M. Li, R. Craigie, M.A. Ditzler, P. Holliger, J.J. DeStefano, Selection of 2'-deoxy-2'-fluoroarabino nucleic acid (FANA) aptamers that bind HIV-1 integrase with picomolar affinity, ACS Chem. Biol. 14 (2019) 2166–2175. https://doi.org/10.1021/acschembio.9b00237.
[34] K. Tanaka, Y. Kasahara, Y. Miyamoto, O. Takumi, T. Kasai, K. Onodera, M. Kuwahara, M. Oka, Y. Yoneda, S. Obika, Development of oligonucleotide-based antagonists of Ebola virus protein 24 inhibiting its interaction with karyopherin alpha 1, Org. Biomol. Chem. 16 (2018) 4456–4463. https://doi.org/10.1039/C8OB00706C.
[35] L. Gold, D. Ayers, J. Bertino, C. Bock, A. Bock, E.N. Brody, J. Carter, A.B. Dalby, B.E. Eaton, T. Fitzwater, D. Flather, A. Forbes, C. Fowler, B. Gawande, M. Goss, M. Gunn, S. Gupta, J. Heil, J. Heilig, B. Hicke, G. Husar, N. Janjic, T. Jarvis,

E. Katilius, T.R. Keeney, N. Kim, T.H. Koch, S. Kraemer, N. Le, D. Levine, W. Lindsey, B. Lollo, W. Mayfield, M. Mehan, S.K. Nelson, M. Nelson, D. Nieuwlandt, M. Nikrad, U. Ochsner, M. Otis, T. Parker, S. Pietrasiewicz, D.I. Resnicow, J. Rohloff, S. Sattin, D. Schneider, B. Singer, M. Stanton, A. Sterkel, S. Stratford, J.D. Vaught, M. Vrkljan, J.J. Walker, M. Watrobka, S. Waugh, A. Weiss, S.K. Wilcox, A. Wolfson, S.K. Wolk, C. Zhang, Aptamer-based multiplexed proteomic technology for biomarker discovery, PLoS One 5 (2010), e15004.

[36] J.H. Park, M.H. Jee, O.S. Kwon, S.J. Keum, S.K. Jang, Infectivity of hepatitis C virus correlates with the amount of envelope protein E2: development of a new aptamer-based assay system suitable for measuring the infectious titer of HCV, Virology 439 (2013) 13–22. https://doi.org/10.1016/j.virol.2013.01.014.

[37] J.J. Trausch, M. Shank-Retzlaff, T. Verch, Development and characterization of an HPV type-16 specific modified DNA aptamer for the improvement of potency assays, Anal. Chem. 89 (2017) 3554–3561. https://doi.org/10.1021/acs.analchem.6b04852.

[38] S.C.B. Gopinath, Y. Sakamaki, K. Kawasaki, P.K.R. Kumar, An efficient RNA aptamer against human influenza B virus hemagglutinin, J. Biochem. 139 (2006b) 837–846. https://doi.org/10.1093/jb/mvj095.

[39] H.-M. Woo, J.-M. Lee, S. Yim, Y.-J. Jeong, Isolation of single-stranded DNA aptamers that distinguish influenza virus hemagglutinin subtype H1 from H5, PLoS One 10 (2015), e0125060. https://doi.org/10.1371/journal.pone.0125060.

[40] S. Lee, Y.S. Kim, M. Jo, M. Jin, D. Lee, S. Kim, Chip-based detection of hepatitis C virus using RNA aptamers that specifically bind to HCV core antigen, Biochem. Biophys. Res. Commun. 358 (2007) 47–52. https://doi.org/10.1016/j.bbrc.2007.04.057.

[41] S.H. Jeon, B. Kayhan, T. Ben-Yedidia, R. Arnon, A DNA aptamer prevents influenza infection by blocking the receptor binding region of the viral hemagglutinin, J. Biol. Chem. 279 (2004) 48410–48419. https://doi.org/10.1074/jbc.M409059200.

[42] S. Yuan, N. Zhang, K. Singh, H. Shuai, H. Chu, J. Zhou, B.K.C. Chow, B.-J. Zheng, Cross-protection of influenza A virus infection by a DNA aptamer targeting the PA endonuclease domain, antimicrob, Agents Chemother. 59 (2015) 4082–4093. https://doi.org/10.1128/AAC.00306-15.

[43] K.M. Pang, D. Castanotto, H. Li, L. Scherer, J.J. Rossi, Incorporation of aptamers in the terminal loop of shRNAs yields an effective and novel combinatorial targeting strategy, Nucleic Acids Res. 46 (2018) e6. https://doi.org/10.1093/nar/gkx980.

[44] M.-L. Andreola, F. Pileur, C. Calmels, M. Ventura, L. Tarrago-Litvak, J.-J. Toulmé, S. Litvak, DNA aptamers selected against the HIV-1 RNase H display *in vitro* antiviral activity, Biochemistry 40 (2001) 10087–10094. https://doi.org/10.1021/bi0108599.

[45] D.J. Schneider, J. Feigon, Z. Hostomsky, L. Gold, High-affinity ssDNA inhibitors of the reverse transcriptase of type 1 human immunodeficiency virus, Biochemistry 34 (1995) 9599–9610. https://doi.org/10.1021/bi00029a037.

[46] M. Labib, A.S. Zamay, D. Muharemagic, A.V. Chechik, J.C. Bell, M.V. Berezovski, Aptamer-based viability impedimetric sensor for viruses, Anal. Chem. 84 (2012) 1813–1816. https://doi.org/10.1021/ac203412m.

[47] F. Chen, Y. Hu, D. Li, H. Chen, X.-L. Zhang, CS-SELEX generates high-affinity ssDNA aptamers as molecular probes for hepatitis C virus envelope glycoprotein E2, PLoS One 4 (2009), e8142. https://doi.org/10.1371/journal.pone.0008142.

[48] H.-R. Liang, G.-Q. Hu, X.-H. Xue, L. Li, X.-X. Zheng, Y.-W. Gao, S.-T. Yang, X.-Z. Xia, Selection of an aptamer against rabies virus: a new class of molecules with antiviral activity, Virus Res. 184 (2014) 7–13. https://doi.org/10.1016/j.virusres.2014.01.021.

[49] B.I. Escudero-Abarca, S.H. Suh, M.D. Moore, H.P. Dwivedi, L.-A. Jaykus, Selection, characterization and application of nucleic acid aptamers for the capture and detection of human norovirus strains, PLoS One 9 (2014), e106805. https://doi.org/10.1371/journal.pone.0106805.

[50] A.G. Leija-Montoya, M.L. Benítez-Hess, J.D. Toscano-Garibay, L.M. Alvarez-Salas, Characterization of an RNA aptamer against HPV-16 L1 virus-like particles, Nucleic Acid Therapeut. 24 (2014) 344–355. https://doi.org/10.1089/nat.2013.0469.

[51] J.M. Binning, T. Wang, P. Luthra, R.S. Shabman, D.M. Borek, G. Liu, W. Xu, D.W. Leung, C.F. Basler, G.K. Amarasinghe, Development of RNA aptamers targeting Ebola virus VP35, Biochemistry 52 (2013) 8406–8419. https://doi.org/10.1021/bi400704d.

[52] S.C.B. Gopinath, K. Hayashi, P.K.R. Kumar, Aptamer that binds to the gD protein of herpes simplex virus 1 and efficiently inhibits viral entry, J. Virol. 86 (2012) 6732–6744. https://doi.org/10.1128/JVI.00377-12.

[53] S.C.B. Gopinath, T.S. Misono, K. Kawasaki, T. Mizuno, M. Imai, T. Odagiri, P.K.R. Kumar, An RNA aptamer that distinguishes between closely related human influenza viruses and inhibits haemagglutinin-mediated membrane fusion, J. Gen. Virol. 87 (2006a) 479–487. https://doi.org/10.1099/vir.0.81508-0.

[54] T. Lakshmipriya, M. Fujimaki, S.C.B. Gopinath, K. Awazu, Generation of anti-influenza aptamers using the systematic evolution of ligands by exponential enrichment for sensing applications, Langmuir 29 (2013) 15107–15115. https://doi.org/10.1021/la4027283.

[55] J. Liu, Y. Yang, B. Hu, Z. Ma, H. Huang, Y. Yu, S. Liu, M. Lu, D. Yang, Development of HBsAg-binding aptamers that bind HepG2.2.15 cells via HBV surface antigen, Virol. Sin. 25 (2010) 27–35. https://doi.org/10.1007/s12250-010-3091-7.

[56] R. Wang, J. Zhao, T. Jiang, Y.M. Kwon, H. Lu, P. Jiao, M. Liao, Y. Li, Selection and characterization of DNA aptamers for use in detection of avian influenza virus H5N1, J. Virol. Methods 189 (2013) 362–369. https://doi.org/10.1016/j.jviromet.2013.03.006.

[57] P. Bellecave, M.-L. Andreola, M. Ventura, L. Tarrago-Litvak, S. Litvak, T. Astier-Gin, Selection of DNA aptamers that bind the RNA-dependent RNA polymerase of hepatitis C virus and inhibit viral RNA synthesis *in vitro*, Oligonucleotides 13 (2003) 455–463. https://doi.org/10.1089/154545703322860771.

[58] Y. Zhang, Z. Yu, F. Jiang, P. Fu, J. Shen, W. Wu, J. Li, Two DNA aptamers against avian influenza H9N2 virus prevent viral infection in cells, PLoS One 10 (2015), e0123060. https://doi.org/10.1371/journal.pone.0123060.

[59] S.H. Kim, J. Lee, B.H. Lee, C.-S. Song, M.B. Gu, Specific detection of avian influenza H5N2 whole virus particles on lateral flow strips using a pair of sandwich-type aptamers, Biosens. Bioelectron. 134 (2019) 123–129. https://doi.org/10.1016/j.bios.2019.03.061.

[60] V.-T. Nguyen, H.B. Seo, B.C. Kim, S.K. Kim, C.-S. Song, M.B. Gu, Highly sensitive sandwich-type SPR based detection of whole H5Nx viruses using a pair of aptamers, Biosens. Bioelectron. 86 (2016) 293–300. https://doi.org/10.1016/j.bios.2016.06.064.

[61] C. Bai, Z. Lu, H. Jiang, Z. Yang, X. Liu, H. Ding, H. Li, J. Dong, A. Huang, T. Fang, Y. Jiang, L. Zhu, X. Lou, S. Li, N. Shao, Aptamer selection and application in multivalent binding-based electrical impedance detection of inactivated H1N1 virus, Biosens. Bioelectron. 110 (2018) 162–167. https://doi.org/10.1016/j.bios.2018.03.047.

[62] I. Hmila, M. Wongphatcharachai, N. Laamiri, R. Aouini, B. Marnissi, M. Arbi, S. Sreevatsan, A. Ghram, A novel method for detection of H9N2 influenza viruses by an aptamer-real time-PCR, J. Virol. Methods 243 (2017) 83–91. https://doi.org/10.1016/j.jviromet.2017.01.024.

[63] W. Li, X. Feng, X. Yan, K. Liu, L. Deng, A DNA aptamer against influenza A virus: an effective inhibitor to the hemagglutinin–glycan interactions, Nucleic Acid Therapeut. 26 (2016) 166–172. https://doi.org/10.1089/nat.2015.0564.

[64] G. Yeom, J. Kang, H. Jang, H.Y. Nam, M.-G. Kim, C.-J. Park, Development of DNA aptamers against the nucleocapsid protein of severe fever with thrombocytopenia syndrome virus for diagnostic application: catalytic signal amplification using replication protein A-conjugated liposomes, Anal. Chem. 91 (2019) 13772–13779. https://doi.org/10.1021/acs.analchem.9b03210.

[65] H.-C. Lai, C.-H. Wang, T.-M. Liou, G.-B. Lee, Influenza A virus-specific aptamers screened by using an integrated microfluidic system, Lab Chip 14 (2014) 2002–2013. https://doi.org/10.1039/C4LC00187G.

[66] S.-L. Hong, M.-Q. Xiang, M. Tang, D.-W. Pang, Z.-L. Zhang, Ebola virus aptamers: from highly efficient selection to application on magnetism-controlled chips, Anal. Chem. 91 (2019) 3367–3373. https://doi.org/10.1021/acs.analchem.8b04623.

[67] Z. Xi, R. Huang, Z. Li, N. He, T. Wang, E. Su, Y. Deng, Selection of HBsAg-specific DNA aptamers based on carboxylated magnetic nanoparticles and their application in the rapid and simple detection of hepatitis B virus infection, ACS Appl. Mater. Interfaces 7 (2015) 11215–11223. https://doi.org/10.1021/acsami.5b01180.

[68] J. Bhardwaj, N. Chaudhary, H. Kim, J. Jang, Subtyping of influenza A H1N1 virus using a label-free electrochemical biosensor based on the DNA aptamer targeting the stem region of HA protein, Anal. Chim. Acta 1064 (2019) 94–103. https://doi.org/10.1016/j.aca.2019.03.005.

[69] K.H. Lee, H. Zeng, Aptamer-based ELISA assay for highly specific and sensitive detection of Zika NS1 protein, Anal. Chem. 89 (2017) 12743–12748. https://doi.org/10.1021/acs.analchem.7b02862.

[70] H. Feng, J. Beck, M. Nassal, K. Hu, A SELEX-screened aptamer of human hepatitis B virus RNA encapsidation signal suppresses viral replication, PLoS One 6 (2011), e27862. https://doi.org/10.1371/journal.pone.0027862.

[71] J.I. Jung, S.R. Han, S.-W. Lee, Development of RNA aptamer that inhibits methyltransferase activity of dengue virus, Biotechnol. Lett. 40 (2018) 315–324. https://doi.org/10.1007/s10529-017-2462-7.

[72] H.-L. Chen, W.-H. Hsiao, H.-C. Lee, S.-C. Wu, J.-W. Cheng, Selection and characterization of DNA aptamers targeting all four serotypes of dengue viruses, PLoS One 10 (2015), e0131240. https://doi.org/10.1371/journal.pone.0131240.

[73] S.K. Choi, C. Lee, K.S. Lee, S.-Y. Choe, I.P. Mo, R.H. Seong, S. Hong, S.H. Jeon, DNA aptamers against the receptor binding region of hemagglutinin prevent avian influenza viral infection, Mol. Cell. 32 (2011) 527–533. https://doi.org/10.1007/s10059-011-0156-x.

[74] H.-M. Kwon, K.H. Lee, B.W. Han, M.R. Han, D.H. Kim, D.-E. Kim, An RNA aptamer that specifically binds to the glycosylated hemagglutinin of avian influenza virus and suppresses viral infection in cells, PLoS One 9 (2014), e97574. https://doi.org/10.1371/journal.pone.0097574.

[75] I. Shiratori, J. Akitomi, D.A. Boltz, K. Horii, M. Furuichi, I. Waga, Selection of DNA aptamers that bind to influenza A viruses with high affinity and broad subtype specificity, Biochem. Biophys. Res. Commun. 443 (2014) 37–41. https://doi.org/10.1016/j.bbrc.2013.11.041.

[76] C. Cheng, J. Dong, L. Yao, A. Chen, R. Jia, L. Huan, J. Guo, Y. Shu, Z. Zhang, Potent inhibition of human influenza H5N1 virus by oligonucleotides derived by SELEX, Biochem. Biophys. Res. Commun. 366 (2008) 670–674. https://doi.org/10.1016/j.bbrc.2007.11.183.

[77] A. Nitsche, A. Kurth, A. Dunkhorst, O. Pänke, H. Sielaff, W. Junge, D. Muth, F. Scheller, W. Stöcklein, C. Dahmen, G. Pauli, A. Kage, One-step selection of Vaccinia virus-binding DNA aptamers by MonoLEX, BMC Biotechnol. 7 (2007) 48. https://doi.org/10.1186/1472-6750-7-48.
[78] F. Tolle, J. Wilke, J. Wengel, G. Mayer, By-product formation in repetitive PCR amplification of DNA libraries during SELEX, PLoS One 9 (2014), e114693. https://doi.org/10.1371/journal.pone.0114693.
[79] Y. Song, J. Song, X. Wei, M. Huang, M. Sun, L. Zhu, B. Lin, H. Shen, Z. Zhu, C. Yang, Discovery of aptamers targeting the receptor-binding domain of the SARS-CoV-2 spike glycoprotein, Anal. Chem. 92 (2020) 9895–9900. https://doi.org/10.1021/acs.analchem.0c01394.
[80] M.V. Berezovski, M.U. Musheev, A.P. Drabovich, J.V. Jitkova, S.N. Krylov, Non-SELEX: selection of aptamers without intermediate amplification of candidate oligonucleotides, Nat. Protoc. 1 (2006) 1359–1369.
[81] M. Berezovski, M. Musheev, A. Drabovich, S.N. Krylov, Non-SELEX selection of aptamers, J. Am. Chem. Soc. 128 (2006) 1410–1411.
[82] A. Kushwaha, Y. Takamura, K. Nishigaki, M. Biyani, Competitive non-SELEX for the selective and rapid enrichment of DNA aptamers and its use in electrochemical aptasensor, Sci. Rep. 9 (2019) 6642.
[83] S. Gao, X. Zheng, B. Jiao, L. Wang, Post-SELEX optimization of aptamers, Anal. Bioanal. Chem. 408 (2016) 4567–4573. https://doi.org/10.1007/s00216-016-9556-2.
[84] M.C. Cowperthwaite, A.D. Ellington, Bioinformatic analysis of the contribution of primer sequences to aptamer structures, J. Mol. Evol. 67 (2008) 95–102. https://doi.org/10.1007/s00239-008-9130-4.
[85] M. Zuker, Mfold web server for nucleic acid folding and hybridization prediction, Nucleic Acids Res. 31 (2003) 3406–3415. https://doi.org/10.1093/nar/gkg595.
[86] J. Akitomi, S. Kato, Y. Yoshida, K. Horii, M. Furuichi, I. Waga, ValFold: program for the aptamer truncation process, Bioinformation 7 (2011) 38–40. https://doi.org/10.6026/97320630007038.
[87] B. Hwang, J.S. Cho, H.J. Yeo, J.-H. Kim, K.M. Chung, K. Han, S.K. Jang, S.-W. Lee, Isolation of specific and high-affinity RNA aptamers against NS3 helicase domain of hepatitis C virus, RNA 10 (2004) 1277–1290.
[88] .S.-J. Cho, H.-M. Woo, K.-S. Kim, J.-W. Oh, Y.-J. Jeong, Novel system for detecting SARS coronavirus nucleocapsid protein using an ssDNA aptamer, J. Biosci. Bioeng. 112 (2011) 535–540. https://doi.org/10.1016/j.jbiosc.2011.08.014.
[89] Y.-W. Zhang, H.-Y. Yan, P. Fu, F. Jiang, Y. Zhang, W.-X. Wu, J.-X. Li, Modified capillary electrophoresis based measurement of the binding between DNA aptamers and an unknown concentration target, Anal. Bioanal. Chem. 405 (2013) 5549–5555. https://doi.org/10.1007/s00216-013-6968-0.
[90] K. Percze, Z. Szakács, É. Scholz, J. András, Z. Szeitner, C.H. van den Kieboom, G. Ferwerda, M.I. de Jonge, R.E. Gyurcsányi, T. Mészáros, Aptamers for respiratory syncytial virus detection, Sci. Rep. 7 (2017) 42794. https://doi.org/10.1038/srep42794.
[91] Z. Zhang, J. Zhang, X. Pei, Q. Zhang, B. Lu, X. Zhang, J. Liu, An aptamer targets HBV core protein and suppresses HBV replication in HepG2.2.15 cells, Int. J. Mol. Med. 34 (2014) 1423–1429. https://doi.org/10.3892/ijmm.2014.1908.
[92] A. Orabi, M. Bieringer, A. Geerlof, V. Bruss, An aptamer against the matrix binding domain on the hepatitis B virus capsid impairs virion formation, J. Virol. 89 (2015) 9281–9287. https://doi.org/10.1128/JVI.00466-15.
[93] C. Chen, Z. Zou, L. Chen, X. Ji, Z. He, Functionalized magnetic microparticle-based colorimetric platform for influenza A virus detection, Nanotechnology 27 (2016) 435102. https://doi.org/10.1088/0957-4484/27/43/435102.
[94] C.-H. Wang, C.-P. Chang, G.-B. Lee, Integrated microfluidic device using a single universal aptamer to detect multiple types of influenza viruses, Biosens. Bioelectron. 86 (2016) 247–254. https://doi.org/10.1016/j.bios.2016.06.071.
[95] C.R. Basso, B.P. Crulhas, M. Magro, F. Vianello, V.A. Pedrosa, A new immunoassay of hybrid nanomater conjugated to aptamers for the detection of dengue virus, Talanta 197 (2019) 482–490. https://doi.org/10.1016/j.talanta.2019.01.058.
[96] T.T. Le, B. Adamiak, D.J. Benton, C.J. Johnson, S. Sharma, R. Fenton, J.W. McCauley, M. Iqbal, A.E.G. Cass, Aptamer-based biosensors for the rapid visual detection of flu viruses, Chem. Commun. 50 (2014) 15533–15536. https://doi.org/10.1039/C4CC07888H.
[97] T.T. Le, P. Chang, D.J. Benton, J.W. McCauley, M. Iqbal, A.E.G. Cass, Dual recognition element lateral flow assay toward multiplex strain specific influenza virus detection, Anal. Chem. 89 (2017) 6781–6786. https://doi.org/10.1021/acs.analchem.7b01149.
[98] C. Wang, L. Zhang, X. Shen, Development of A nucleic acid lateral flow strip for detection of hepatitis C virus (hcv) core antigen, Nucleos Nucleot. Nucleic Acids 32 (2013) 59–68. https://doi.org/10.1080/15257770.2013.763976.
[99] Y. Pang, Z. Rong, J. Wang, R. Xiao, S. Wang, A fluorescent aptasensor for H5N1 influenza virus detection based-on the core–shell nanoparticles metal-enhanced fluorescence (MEF), Biosens. Bioelectron. 66 (2015) 527–532. https://doi.org/10.1016/j.bios.2014.10.052.
[100] R. Yamamoto, P.K.R. Kumar, Molecular beacon aptamer fluoresces in the presence of Tat protein of HIV-1, Gene Cell. 5 (2000) 389–396. https://doi.org/10.1046/j.1365-2443.2000.00331.x.
[101] R. Huang, Z. Xi, Y. Deng, N. He, Fluorescence based Aptasensors for the determination of hepatitis B virus e antigen, Sci. Rep. 6 (2016) 31103. https://doi.org/10.1038/srep31103.
[102] X. Weng, S. Neethirajan, Aptamer-based fluorometric determination of norovirus using a paper-based microfluidic device, Microchim. Acta 184 (2017) 4545–4552. https://doi.org/10.1007/s00604-017-2467-x.
[103] N. Lee, C. Wang, J. Park, User-friendly point-of-care detection of influenza A (H1N1) virus using light guide in three-dimensional photonic crystal, RSC Adv. 8 (2018) 22991–22997. https://doi.org/10.1039/C8RA02596G.
[104] L. Xu, R. Wang, L.C. Kelso, Y. Ying, Y. Li, A target-responsive and size-dependent hydrogel aptasensor embedded with QD fluorescent reporters for rapid detection of avian influenza virus H5N1, Sensor. Actuator. B Chem. 234 (2016) 98–108. https://doi.org/10.1016/j.snb.2016.04.156.
[105] S.-K. Suh, S. Song, H.-B. Oh, S.-H. Hwang, S.S. Hah, Aptamer-based competitive binding assay for one-step quantitation of hepatitis B surface antigen, Analyst 139 (2014) 4310–4314. https://doi.org/10.1039/C4AN00619D.
[106] B. Kim, K.W. Chung, J.H. Lee, Non-stop aptasensor capable of rapidly monitoring norovirus in a sample, J. Pharmaceut. Biomed. Anal. 152 (2018) 315–321. https://doi.org/10.1016/j.jpba.2018.02.022.
[107] H. Bai, R. Wang, B. Hargis, H. Lu, Y. Li, A SPR aptasensor for detection of avian influenza virus H5N1, Sensors 12 (2012) 12506–12518. https://doi.org/10.3390/s120912506.
[108] T. Lee, G.H. Kim, S.M. Kim, K. Hong, Y. Kim, C. Park, H. Sohn, J. Min, Label-free localized surface plasmon resonance biosensor composed of multi-functional DNA 3 way junction on hollow Au spike-like nanoparticles (HAuSN) for avian influenza virus detection, Colloids Surf. B Biointerfaces 182 (2019) 110341. https://doi.org/10.1016/j.colsurfb.2019.06.070.
[109] V.I. Kukushkin, N.M. Ivanov, A.A. Novoseltseva, A.S. Gambaryan, I.V. Yaminsky, A.M. Kopylov, E.G. Zavyalova, Highly sensitive detection of influenza virus with SERS aptasensor, PLoS One 14 (2019), e0216247. https://doi.org/10.1371/journal.pone.0216247.
[110] J. Kwon, Y. Lee, T. Lee, J.-H. Ahn, Aptamer-based field-effect transistor for detection of avian influenza virus in chicken serum, Anal. Chem. 92 (2020) 5524–5531. https://doi.org/10.1021/acs.analchem.0c00348.
[111] K.H. Cho, D.H. Shin, J. Oh, J.H. An, J.S. Lee, J. Jang, Multidimensional conductive nanofilm-based flexible aptasensor for ultrasensitive and selective HBsAg detection, ACS Appl. Mater. Interfaces 10 (2018) 28412–28419. https://doi.org/10.1021/acsami.8b09918.
[112] M.F. Fatin, A. Rahim Ruslinda, S.C.B. Gopinath, M.K.Md Arshad, High-performance interactive analysis of split aptamer and HIV-1 Tat on multiwall carbon nanotube-modified field-effect transistor, Int. J. Biol. Macromol. 125 (2019) 414–422. https://doi.org/10.1016/j.ijbiomac.2018.12.066.
[113] A. Rahim Ruslinda, K. Tanabe, S. Ibori, X. Wang, H. Kawarada, Effects of diamond-FET-based RNA aptamer sensing for detection of real sample of HIV-1 Tat protein, Biosens, Bioelectron 40 (2013) 277–282. https://doi.org/10.1016/j.bios.2012.07.048.
[114] K. Kiilerich-Pedersen, J. Daprà, S. Cherré, N. Rozlosnik, High sensitivity point-of-care device for direct virus diagnostics, Biosens. Bioelectron. 49 (2013) 374–379. https://doi.org/10.1016/j.bios.2013.05.046.
[115] J. Lum, R. Wang, B. Hargis, S. Tung, W. Bottje, H. Lu, Y. Li, An impedance aptasensor with microfluidic chips for specific detection of H5N1 avian influenza virus, Sensors 15 (2015) 18565–18578. https://doi.org/10.3390/s150818565.
[116] K. Ghanbari, M. Roushani, A. Azadbakht, Ultra-sensitive aptasensor based on a GQD nanocomposite for detection of hepatitis C virus core antigen, Anal. Biochem. 534 (2017) 64–69. https://doi.org/10.1016/j.ab.2017.07.016.
[117] J.-M. Lee, J. Kim, I. Ryu, H.-M. Woo, T.G. Lee, W. Jung, S. Yim, Y.-J. Jeong, An aptamer-based electrochemical sensor that can distinguish influenza virus subtype H1 from H5, J. Microbiol. Biotechnol. 27 (2017) 2037–2043. https://doi.org/10.4014/jmb.1708.08015.
[118] K. Ghanbari, M. Roushani, A nanohybrid probe based on double recognition of an aptamer MIP grafted onto a MWCNTs-Chit nanocomposite for sensing hepatitis C virus core antigen, Sensor. Actuator. B Chem. 258 (2018) 1066–1071. https://doi.org/10.1016/j.snb.2017.11.145.
[119] F. Chekin, K. Bagga, P. Subramanian, R. Jijie, S.K. Singh, S. Kurungot, R. Boukherroub, S. Szunerits, Nucleic aptamer modified porous reduced graphene oxide/MoS2 based electrodes for viral detection: application to human papillomavirus (HPV), Sensor. Actuator. B Chem. 262 (2018) 991–1000. https://doi.org/10.1016/j.snb.2018.02.065.
[120] T. Lee, S.Y. Park, H. Jang, G.-H. Kim, Y. Lee, C. Park, M. Mohammadniaei, M.-H. Lee, J. Min, Fabrication of electrochemical biosensor consisted of multi-functional DNA structure/porous au nanoparticle for avian influenza virus (H5N1) in chicken serum, Mater. Sci. Eng. C 99 (2019) 511–519. https://doi.org/10.1016/j.msec.2019.02.001.
[121] F.S. Diba, S. Kim, H.J. Lee, Amperometric bioaffinity sensing platform for avian influenza virus proteins with aptamer modified gold nanoparticles on carbon chips, Biosens. Bioelectron. 72 (2015) 355–361. https://doi.org/10.1016/j.bios.2015.05.020.
[122] R. Wang, L. Xu, Y. Li, Bio-nanogate controlled enzymatic reaction for virus sensing, Biosens. Bioelectron. 67 (2015) 400–407. https://doi.org/10.1016/j.bios.2014.08.071.
[123] R. Wang, L. Wang, Z.T. Callaway, H. Lu, T.J. Huang, Y. Li, A nanowell-based QCM aptasensor for rapid and sensitive detection of avian influenza virus, Sensor. Actuator. B Chem. 240 (2017) 934–940. https://doi.org/10.1016/j.snb.2016.09.067.
[124] R. Wang, Y. Li, Hydrogel based QCM aptasensor for detection of avian influenzavirus, Biosens. Bioelectron. 42 (2013) 148–155. https://doi.org/10.1016/j.bios.2012.10.038.
[125] M. Minunni, S. Tombelli, A. Gullotto, E. Luzi, M. Mascini, Development of biosensors with aptamers as bio-recognition element: the case of HIV-1 Tat protein, Biosens. Bioelectron. 20 (2004) 1149–1156. https://doi.org/10.1016/j.bios.2004.03.037.